

Parametric Study of Leading-Edge Slat Size and Placement  
Parameters for achieving optimal Aerodynamic and Acoustic  
Performance of VAWT



Author

MUHAMMAD BILAL MASOOD

Reg Number

00000170818

Supervisor

Dr. Emad Uddin

DEPARTMENT: SCHOOL OF MECHANICAL & MANUFACTURING  
ENGINEERING

NATIONAL UNIVERSITY OF SCIENCES AND TECHNOLOGY

ISLAMABAD

JULY , 2020

Parametric Study of Leading-Edge Slat Size and Placement  
Parameters for achieving optimal Aerodynamic and Acoustic  
Performance of VAWT

Author


MUHAMMAD BILAL MASOOD

Reg Number

00000170818

A thesis submitted in partial fulfillment of the requirements for the degree of  
MS Mechanical Engineering

Thesis Supervisor: Dr. Emad Uddin

Thesis Supervisor's Signature:  \_\_\_\_\_

DEPARTMENT  
SCHOOL OF MECHANICAL & MANUFACTURING ENGINEERING  
NATIONAL UNIVERSITY OF SCIENCES AND TECHNOLOGY,  
ISLAMABAD  
JULY, 2020


# National University of Sciences & Technology

## MASTER THESIS WORK

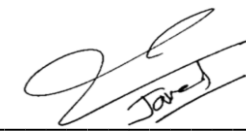
We hereby recommend that the dissertation prepared under our supervision by : Muhammad Bilal Masood Reg. No. 170818 Titled: Parametric study of Leading-Edge Slat Size and Placement Parameters for achieving optimal Aerodynamic and Acoustic Performance of VAWT be accepted in partial fulfillment of the requirements for the award of MS Mechanical Engineering degree.

### Examination Committee Members

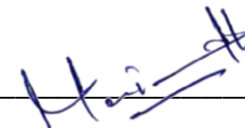
1. Name: Dr. Muhammad Sajid

Signature: 

2. Name: Dr. Adeel Javed

Signature: 

3. Name: Dr. Zaib Ali

Signature: 

Supervisor's name: Dr. Emad Uddin

Signature: 

Date: 17/07/2020



Head of Department

Date

**COUNTERSIGNED**

Date: \_\_\_\_\_

\_\_\_\_\_  
Dean/Principal

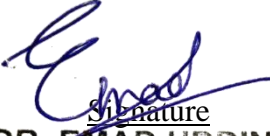
## **Certificate for Plagiarism**

It is certified that MS Thesis Titled: Parametric Study of Leading-Edge Slat Size and Placement Parameters for achieving optimal Aerodynamic and Acoustic Performance of VAWT by M BILAL MASOOD has been examined by us. We undertake the follows:

- a. Thesis has significant new work/knowledge as compared already published or are under consideration to be published elsewhere. No sentence, equation, diagram, table, paragraph or section has been copied verbatim from previous work unless it is placed under quotation marks and duly referenced.
- b. The work presented is original and own work of the author (i.e. there is no plagiarism). No ideas, processes, results or words of others have been presented as Author own work.
- c. There is no fabrication of data or results which have been compiled/analyzed.
- d. There is no falsification by manipulating research materials, equipment or processes, or changing or omitting data or results such that the research is not accurately represented in the research record.
- e. The thesis has been checked using TURNITIN (copy of originality report attached) and found within limits as per HEC plagiarism Policy and instructions issued from time to time.

### **Name & Signature of Supervisor**

**Dr. Emad Uddin**

  
Signature  
**DR. EMAD UDDIN**  
HoD Mech Engg.  
School of Mechanical &  
Manufacturing Engineering (SMME)  
NUST, H-12, Islamabad

## **THESIS ACCEPTANCE CERTIFICATE**

Certified that final copy of MS thesis written by Mr. M BILAL MASOOD, Registration No 00000170818, of SMME has been vetted by undersigned, found complete in all respects as per NUST Statutes/Regulations, is free of plagiarism, errors and mistakes and is accepted as partial fulfillment for award of MS degree. It is further certified that necessary amendments as pointed out by GEC members of the scholar have also been incorporated in the said thesis.

Signature: \_\_\_\_\_ 

Name of Supervisor: Dr. Emad Uddin

Date: \_\_\_\_\_

Signature (HOD): \_\_\_\_\_ 

Date: \_\_\_\_\_

Signature (Dean/Principal): \_\_\_\_\_

Date: \_\_\_\_\_

## **Declaration**

I certify that this research work titled “*Parametric Study of Leading-Edge Slat Size and Placement Parameters for achieving optimal Aerodynamic and Acoustic Performance of VAWT*” is my own work. The work has not been presented elsewhere for assessment. The material that has been used from other sources it has been properly acknowledged / referred.



Signature of Student

Muhammad Bilal Masood

2016-NUST-MS-Mech-00000170818

## **Plagiarism Certificate (Turnitin Report)**

This thesis has been checked for Plagiarism. Turnitin report endorsed by Supervisor is attached.



Signature of Student

Muhammad Bilal Masood  
2016-NUST-MS-Mech-00000170818



Signature of Supervisor

## **Copyright Statement**

- Copyright in text of this thesis rests with the student author. Copies (by any process) either in full, or of extracts, may be made only in accordance with instructions given by the author and lodged in the Library of NUST School of Mechanical & Manufacturing Engineering (SMME). Details may be obtained by the Librarian. This page must form part of any such copies made. Further copies (by any process) may not be made without the permission (in writing) of the author.
- The ownership of any intellectual property rights which may be described in this thesis is vested in NUST School of Mechanical & Manufacturing Engineering, subject to any prior agreement to the contrary, and may not be made available for use by third parties without the written permission of the SMME, which will prescribe the terms and conditions of any such agreement.
- Further information on the conditions under which disclosures and exploitation may take place is available from the Library of NUST School of Mechanical & Manufacturing Engineering, Islamabad.



## **Acknowledgements**

I am thankful to my Creator Allah Subhana-Watala to have guided me throughout this work at every step and for every new thought which You setup in my mind to improve it. Indeed, I could have done nothing without Your priceless help and guidance. Whosoever helped me throughout the course of my thesis, whether my parents or any other individual was Your will, so indeed none be worthy of praise but You.

I am profusely thankful to my beloved parents who raised me when I was not capable of walking and continued to support me throughout in every department of my life.

I would also like to express special thanks to my supervisor Dr. Emad Uddin for his help throughout my thesis. I can safely say that I haven't learned any other engineering subject in such depth than the ones which he has taught.

I would also like to pay special thanks to my wife for her tremendous support and cooperation. I appreciate her patience and support throughout the whole thesis.

Finally, I would like to express my gratitude to all the individuals who have rendered valuable assistance to my study.

*Dedicated to my beloved parents, sister, brother and my wife for their prayers, cooperation and support which led me to this wonderful achievement.*

## Abstract

Nowadays, small VAWT are receiving more consideration due to their appropriateness in micro-electricity production. Different techniques have been used to improve the efficiency of power. Presently parametric study of leading-edge slat size and placement parameters is conducted to achieve optimum aerodynamic and acoustic performance of VAWT. To validate the methodology, CFD results of 2D AEOLOS VAWT at Tip speed Ratio ( $\lambda$ ) of 2.094 are compared with that of OEM provided performance data. Afterwards, acoustic analysis was carried out and results are in good comparison with the technical specification of AEOLOS (1kW) VAWT. Coefficient of Moment  $C_m$ , and Coefficient of Power  $C_P$ , are studied in Ansys Fluent® using unsteady Reynolds- averaged Navier-Stokes (URANS) and turbulence is modeled using improved three equation transition (SST) model. The noise (A- weighted Sound Pressure Level) radiated from VAWT is calculated using the FW-H acoustic codes. Results of the study indicate that minimum overlapping between the main and slat aerofoil is desirable and slat placement angle ( $\beta$ ) must be selected less than  $15^\circ$ . As far as slat size is considered there must be a tradeoff between desired aerodynamic performance and acoustic noise level.

**Keywords:** CFD, Tip Speed Ratio, Solidity, Leading Edge Slat

# Table of Contents

<b>DECLARATION</b> .....	<b>I</b>
<b>PLAGIARISM CERTIFICATE (TURNITIN REPORT)</b> .....	<b>II</b>
<b>COPYRIGHT STATEMENT</b> .....	<b>III</b>
<b>ACKNOWLEDGEMENTS</b> .....	<b>IV</b>
<b>ABSTRACT</b> .....	<b>VI</b>
<b>TABLE OF CONTENTS</b> .....	<b>VII</b>
<b>LIST OF FIGURES</b> .....	<b>IX</b>
<b>LIST OF TABLES</b> .....	<b>X</b>
<b>1. INTRODUCTION</b> .....	<b>1</b>
1.1 WIND TURBINE .....	1
1.2 VERTICAL AXIS WIND TURBINE .....	1
<b>2. LITERATURE REVIEW</b> .....	<b>1</b>
<b>3. NUMERICAL SETTING</b> .....	<b>3</b>
3.1. GEOMETRY AND TECHNICAL DETAILS OF VAWT .....	3
3.2. SLAT DESIGN .....	5
3.3. NUMERICAL DOMAIN AND GRID .....	6
3.4. SOLUTION METHODS AND CONTROLS.....	8
3.5. ACOUSTIC MODELING.....	9
<b>4. VALIDATION STUDY</b> .....	<b>10</b>
4.1. VERIFICATION AND VALIDATION OF SOLUTION .....	10
4.2. ACOUSTIC VALIDATION .....	12
<b>5. AERODYNAMIC AND ACOUSTIC BEHAVIOR OF VAWT WITH SLAT</b> .....	<b>13</b>
5.1. NUMERICAL SETTING.....	13
5.2 AERODYNAMICS OF SLATED VAWT.....	13
5.3 ACOUSTIC OF VAWT.....	20
5.4. PERFORMANCE ANALYSIS OF VAWT WITH SLAT .....	21
5.4.1 Behavior of instantaneous moment curve.....	23
5.4.2 Effect of Distance between slat aerofoil trailing edge and Leading Edge of Main Aerofoil in X- direction (XTE) on Coefficient of moment. ....	24
5.4.3 Effect of Slat Angle ( $\beta$ ) .....	24
5.4.4 Effect of Slat Size ( $C_s$ ).....	25

5.4.5 Sound Pressure Level .....	25
5.4.6 Vorticity Curve of Case with Slat angle $10^\circ$ & $20^\circ$ .....	26
<b>6. DISCUSSION</b> .....	<b>28</b>
6.1 RECOMMENDATION FOR FUTURE WORK .....	28
<b>7. CONCLUSION</b> .....	<b>29</b>
<b>REFERENCES:</b> .....	<b>30</b>

## List of Figures

FIGURE 1: ASSEMBLY DRAWING OF AEOLOS -V .....	4
FIGURE 2: <i>ILLUSTRATING OF SLAT PLACEMENT PARAMETERS</i> .....	6
FIGURE 3: DOMAIN SIZING .....	7
FIGURE 4: COMPUTATIONAL GRID (A) NEAR ROTATING ZONE (B) NEAR AEROFOIL .....	8
FIGURE 5: COMPUTATIONAL GRID (A) NEAR ROTATING ZONE (B) NEAR AEROFOIL AND SLAT .....	8
FIGURE 6 (A): COEFFICIENT OF MOMENT AS A FUNCTION OF AZIMUTH ANGLE FOR VAWT. (B) COEFFICIENT OF MOMENT OF SINGLE BLADE AS A FUNCTION OF AZIMUTH ANGLE .....	11
FIGURE 7 (A) SPL AS FUNCTION OF AZIMUTH ANGLE, AND (B) TSPL AS FUNCTION OF FREQUENCY .....	12
FIGURE 8: COEFFICIENT OF MOMENT AT DIFFERENT SLAT ANGLES AND $X_{TE}$ AS FUNCTION OF AZIMUTH ANGLE (A) SLAT SIZE 135 MM, (B) SLAT SIZE 180 MM, (C) SLAT SIZE 225 MM .....	19
FIGURE 9: CM & SPL (DB A) AS A FUNCTION OF SLAT ANGLE (A) SLAT SIZE 135, $X_{TE}$ =47.25, 56.25, 69.75 MM, (B) SLAT SIZE 180, $X_{TE}$ =47.25, 56.25, 69.75 MM, (C) SLAT SIZE 225, $X_{TE}$ =47.25, 56.25, 69.75 MM .....	23
FIGURE 10: SOUND PRESSURE LEVEL AS FUNCTION OF AZIMUTH ANGLE (A) DIRECTIVITY PLOT OF A-WEIGHTED SPL (B) TSPL PLOT AT $x/R = 1.25, 1.75, 2$ .....	26
FIGURE 11: VORTICITY CONTOURS OF ( $C_s = 180, X_{TE} = 47.25$ MM, $B = 10^\circ$ ) AT MAX (A) AND MIN (B) PERFORMANCE .....	27
FIGURE 12: VORTICITY CONTOURS OF ( $C_s = 180, X_{TE} = 47.25$ MM, $B = 20^\circ$ ) AT MAX (A) AND MIN (B) PERFORMANCE .....	28

# List of Tables

TABLE 1: GEOMETRICAL, OPERATIONAL AND TECHNICAL CHARACTERISTIC OF AEOLOS-V .....	5
TABLE 2: DETAIL OF SLAT CHORD .....	5
TABLE 3: DETAILS OF SLAT PLACEMENT PARAMETERS .....	6
TABLE 4: DOMAIN SIZE .....	7
TABLE 5: MESH INDEPENDENCE STUDY FOR REFERENCE CASE.....	11
TABLE 6: TIME STEP INDEPENDENCE STUDY FOR REFERENCE CASE.....	11
TABLE 7 COMPARISON OF COEFFICIENT OF POWER.....	12
TABLE 8 : MESH INDEPENDENCE STUDY FOR VAWT WITH SLAT.....	13
TABLE 9: AVERAGE VALUE OF MOMENT COEFFICIENT AND MAXIMUM VALUE OF SOUND PRESSURE LEVEL (SPL DB A) AT X/R 1.25 .....	20
TABLE 10: COMPARISON OF MOMENT COEFFICIENT .....	25

# 1. Introduction

## 1.1 Wind Turbine

World is facing major energy challenges. Due to the rising pressure on energy resources world is shifting from fossil fuel to renewable energies. Wind energy is abundantly available resource. Wind turbines mainly are of two types: vertical axis (VAWT) and horizontal axis (HAWT). HAWT are the most common type of wind turbines built across the world. VAWT is a type of wind turbine which have two or three blades and in which the main rotor shaft runs vertically.

## 1.2 Vertical Axis Wind Turbine

The most popular type of turbine is vertical axis turbine people are adding to make their home source of renewable energy is Vertical Axis Wind Turbine (VAWT). They are not as common as HAWT however, due to their compact size they are getting more attention. VAWTs are mostly of two types:

- Savonius
- Darrieus

**a. Savonius Turbine.** It has slowed rotating speed and high torque. It is used in highly reliable and have low in power efficiency. They mostly use airfoil shape lift generating blade to rotate the rotor, the Savonius uses drag and therefore cannot rotate faster than the approaching wind speed.

**b. Darrieus Turbine.** It was named after its inventor Georges Darrieus who invented it in 1931. It has high rotational speed and low torque turbine. Due to its low starting torque it requires manual push to start turning its rotor.

## 2. Literature Review

Nowadays performance of wind turbine is measured using two approaches 1) Observational / Experimental Approach 2) Numerical / Simulation Approach. Experimental Approaches include physically sensing the performance parameters of the wind turbine. Second one uses



computational tools for measuring the performance parameters it also reduces the man hours. CFD simulations results are validated by experimental results. It can solve complex flow behavior and same can also be visualize for better understanding. Such techniques will provide better prediction for improvement of design. Literature provides an insight about wind turbine as this is the field which requires former results to validate CFD results and simulation.

There are numerous kinds of CFD models being used for the simulating complex flow physics of wind turbine. These models are generally known as CFD models. Input and boundary conditions can be sued from the mesoscale. Turbulence model parameterized and it depends on the CFD model: LES, hybrid URANS/LES, URANS or steady RANS.

VAWTs have gained interest due to their compactness and adaptability for urban installation (1–3). Despite low power generation, Vertical Axis Wind turbine are gaining more suit ability for installation in urban area due to compact size and easy to install in urban area. The omni directional capability, low installation and maintenance cost are few of the main advantages of Vertical axis turbine over their Horizontal Axis counterparts. VAWT have certain disadvantages such as low power efficiency and self-starting issues as compared to HAWT.

For improving the aerodynamic performance of VAWT number of studies have been conducted by employing various flow control devices such as gunnery flap, leading edge slot etc for improving the power coefficient of turbine. Improving the performance of Vertical Axis Turbine using high lift devices is the area of interest these days. Previously Gauana et al (4) studied the aerodynamics characteristic of double element aerofoil on HAWT. The result of study indicates a considerable increase in the coefficient of lift, however the acoustic analysis of VAWT has not been initiated.

It is noteworthy that the acoustic pollution is the major disadvantage of wind turbine for their usage in the developed area. Noise radiated from wind turbine is divided in to two categories. First category is mechanical noise, it is produced by auxiliary equipment, cooling fans, yaw drives, generator, and gearbox and aerodynamic noises which are dependent on interaction of turbulence with the blade surfaces (5). It is important to study the noise radiated from the blades of turbine. With the advancement of Computational Fluid Dynamics tools, accurate prediction of VAWT simulation is possible. Tadamsa and zangneh (6) has accurately predicted the aerodynamics and noise emitted from the HAWT using RANS approach and transition turbulence model coupled with Ffowcs Williams -Hawaking (FW-H) equation. The result of this

study has correctly predicted the relation between intensity of radiated noise and rotational speed of turbine.

Due to the limited information about the design and placement of slat for employment on VAWT for enhancing its performance. In present paper a parametric study is conducted on the slat design parameters i.e slat size, slat placement angle ( $\beta$ ) and distance of slat trailing edge from the leading edge of main aerofoil XTE. Slat of various sizes have been selected and their aerodynamic behavior is studied on different slat placement parameters. Similarly, acoustic analysis has also been carried out for selecting the optimized slat size for its employment on VAWT. The study has been conducted at one tip speed ratio  $\lambda$  (2.094).

Accurate prediction of aerodynamics performance of VAWT using computational fluid dynamics require appropriately fine azimuth increase ( $d\theta$ ) and resolution of grid to capture the important flow details. In present study, 2D aerodynamic analysis of Aeolos (1kW) VAWT is carried out and validated with experimental data of Aeolos (1kW) VAWT and baseline case of (7). Good agreement has been observed in calculated and experimental value of power coefficient. In comparison to  $C_p$  value of baseline case of (7) 3.3% improvement in calculated  $C_p$  value has been observed by employing improved turbulence model and fine Azimuth increment ( $d\theta$ ) of  $0.5^\circ$  to capture the flow dynamics at tip speed ratio ( $\lambda$ ) 2.094. Acoustic behavior is captured by Ffowcs Williams -Hawking (FW-H) equation. Total of 108 receivers have been placed in circular array (36 receiver each) at distance  $x/R = 1.25, 1.75, 2$  from turbine rotor. Methodology employed in validation study have been used for studying the aerodynamic and acoustic behavior of slat. To achieve the accurate results of CFD azimuth augmentation, size of domain and criteria of convergence defined by Rezaeiha et al. (8,9) were used.

### **3. Numerical Setting**

#### **3.1. Geometry and Technical Details of VAWT**

Performance analysis of H-type Aeolos-V (1kW) VAWT is conducted by utilizing CFD tool. The diameter ( $D$ ) of turbine is 2 m and diameter of shaft is 0.36 m. The shaft and turbine rotate counterclockwise and have similar speed of rotation. The free stream velocity ( $U_\infty$ ) 10 m/sec is used in current study. Chord base Reynolds Number  $Re_c$  is 670,000. The Aeolos-V (1kW) turbine has solidity ( $\sigma$ ) of 0.675, aerofoil chord length ( $c$ ) of 0.45 m. Current study is performed at fixed turbine rotational speed ( $\Omega$ ) 20 rad/s or 200 RPM, which leads to the tip speed ratio ( $\lambda$ ) of 2.094. Equation 1 and 2 are used for defining the Tip speed ratio and solidity of turbine. Key geometrical, operational and technical characteristics of the Aeolos-V (1kW) turbine are defined

in Table 1. These characteristics are same as provided by OEM. The assembly drawing and commercially available Aeolos-V (1kW) VAWT is depicted in Figure 1.

$$\Lambda = R\Omega / U_{\infty} \quad (1)$$

$$\sigma = nc / d \quad (2)$$

$n$  is the number of blades;  $c$  is the chord length of aerofoil and  $d$  is the diameter of turbine.

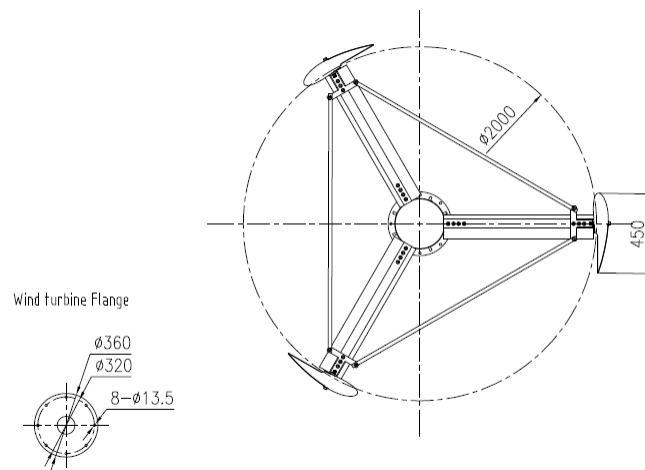


*Figure 1: Assembly Drawing of Aeolos -V*

Parameter	Value	Parameter	Value
Number of Blade (n)	3	Blade Aspect Ratio (H/c)	6.22
Diameter (d)	2 m	Shaft Diameter (d <sub>s</sub> )	0.36 m
Swept Area (A)	5.6 m <sup>2</sup>	Tip Speed Ratio ( $\lambda$ )	2.094
Aerofoil	OEM Provided	Free Stream Velocity (U $\infty$ )	10 m/s
Aerofoil Chord (c)	450 mm	Turbulence intensity	5%
Solidity ( $\sigma$ )	0.675	Rotational Speed	20 rad/ sec
Density ( $\rho$ )	1.1845 Kg/ m <sup>3</sup>	Viscosity	1.844 *10 <sup>-5</sup> kg/ms

Table 1: Geometrical, Operational and Technical Characteristic of Aeolos-V

### 3.2. Slat Design

Presently parametric study of slat size and slat positioning parameters on the performance of the VAWT is studied. Slat aerofoil of same aerodynamics characteristic as of main aerofoil is chosen. The working principle of slat and main aerofoil is based on multi-element aerofoil knowledge and is described in detail in (4,10). Slat size in the current study are chosen in accordance with the result of (1).

SNo	C <sub>s</sub> /C <sub>m</sub>	Chord of Main Aerofoil (C <sub>m</sub> ) mm	Chord length of Slat Aerofoil (C <sub>s</sub> ) mm
1	0.3	450	135
2	0.4	450	180
3	0.5	450	225

Table 2: Detail of Slat Chord

Details of slat chord length is tabulated in Table 2. The placement of the slat trailing edge (TE) & angle of slat aerofoil are the critical factors of slat design.

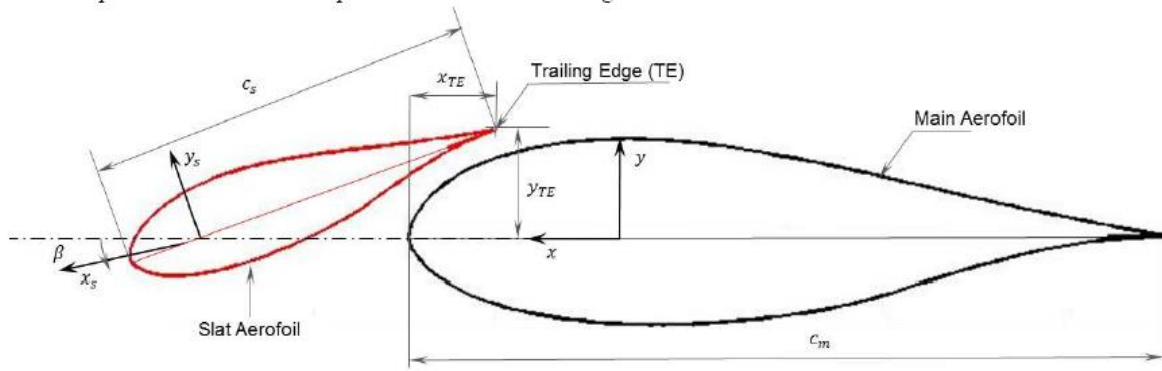


Figure 2: Illustrating of Slat Placement Parameters

The placement of the slat aerofoil trailing edge (TE) & angle of slat aerofoil regarding main aerofoil are two critical factors of slat design. These design factors are defined by three important parameters which are defined below and illustrated in Figure 2.

- X-orientation of slat aerofoil trailing edge (TE) is denoted by ( $X_{TE}$ )
- Y-Orientation of slat aerofoil trailing edge (TE) is denoted by ( $Y_{TE}$ ).
- The angle of the slat aerofoil chord with X-direction is represented by Slat placement angle ( $\beta$ ). Nose up direction is positive.

Slat placement parameter are chosen as per the result of (4,10). Behavior of VAWT with Slat was studied by placing the Trailing Edge (TE) of slat aerofoil at 10.5 %, 12.5% and 15.5 % of chord length of main aerofoil ( $C_m$ ) respectively. In present study a total of 27 cases each were formulated for analyzing the effect of slat size and placement parameters on the performance of VAWT. Details of parameters is tabulated in Table 3

S No	$X_{TE}$ (mm)	$\beta$ (deg)
a	47.25	-10
b	47.25	-15
c	47.25	-20
d	56.25	-10
e	56.25	-15
f	56.25	-20
g	69.75	-10
h	69.75	-15
i	69.75	-20

Table 3: Details of Slat Placement Parameters

### 3.3. Numerical Domain and Grid

In this study two-dimensional (2-D) domain is utilized as illustrated in Figure 3. Note that on the basis of comprehensive study and sensitivity analysis of 2 D and 2.5 D computational domain of (8,9) a 2D computational domain is selected. This domain is selected on the midplane of turbine to minimize the 3D tip effect (12). Aeolos VAWT has blade aspect ratio of 6.22. It was inferred

from the finding of previous CFD simulations of VAWTs that a minimum domain width of  $20d$  is required for minimizing the effect of blockage ratio and side boundaries (to less than 5%) same is discussed in detail at (9). For 2-D simulations blockage ratio is defined as  $d/W$  where  $d$  is the diameter of the turbine and  $W$  is the domain width. In present study a minimum domain size of  $20d$  was employed whereas the diameter of the rotational core ( $d_c$ ) is selected as  $1.5d$  on the basis of the results of (9). The sliding grid interface is employed to join the rotating core with the surrounding fixed domain. Undermentioned computational parameters are employed in this study: Distance of domain inlet to the turbine center is represented by ( $d_i$ )

- Similarly, distance of domain outlet ( $d_o$ ) for the current study are  $5D$ ,  $25D$ , respectively.
- Plane of rotation of the blades is defined as per the finding of (12) as shown in Figure 3. Everywhere the computational grid is made up of triangular cells. The maximum value of cell skewness in the grid is 0.65 and the minimum orthogonal quality is 0.35. The  $y^+$  values is maintained to  $\leq 1$ , The total number of cells for reference case are approximately 3.4 million. Figure. 4 & 5 shows the computational grid and parameters are mentioned in Table 4.
- The uniform velocity inlet, pressure outlet, symmetry sides and no slip walls boundary condition is selected. The turbulence length scale at inlet and outlet is selected on the basis of length scale of interest in this case it is equal to turbine diameter 2m.

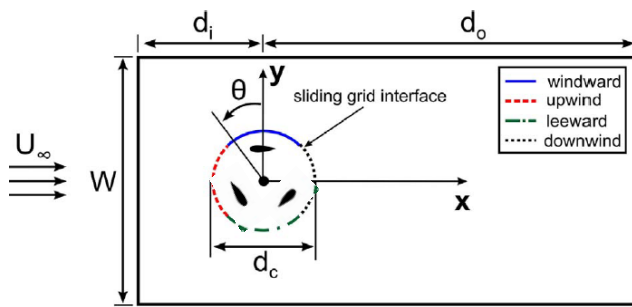


Figure 3: Domain Sizing

Parameter	Value
Diameter (D)	2 m
Domain Inlet ( $d_i$ )	7.5 D
Domain Outlet ( $d_o$ )	25 D
Width (W)	20 D
Domain Rotating ( $d_c$ )	1.5 D
<i>Table 4: Domain Size</i>	

Computational grid near the rotating zone and near aerofoil for the reference case and cases of slatted VAWT is shown in Figure 4 and Figure 5 respectively.

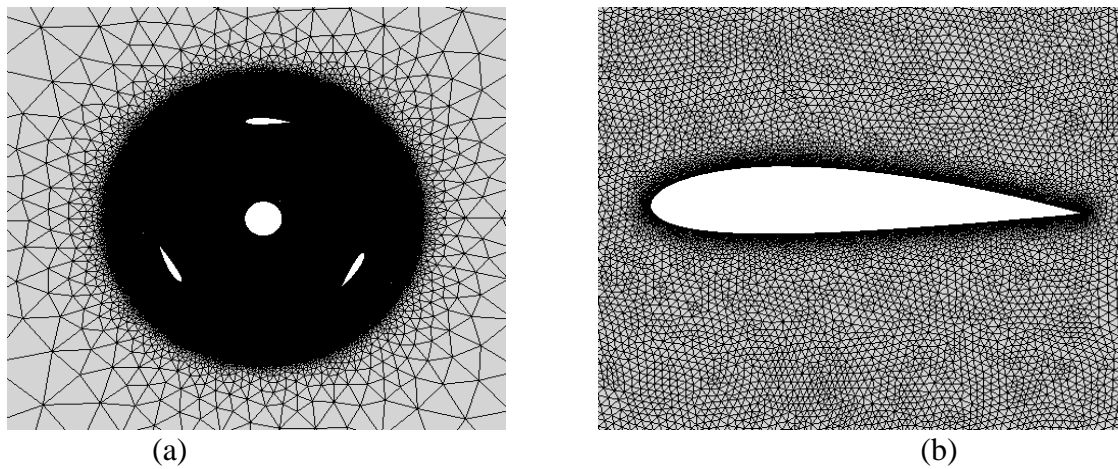


Figure 4: Computational Grid (a) near Rotating Zone (b) near aerofoil

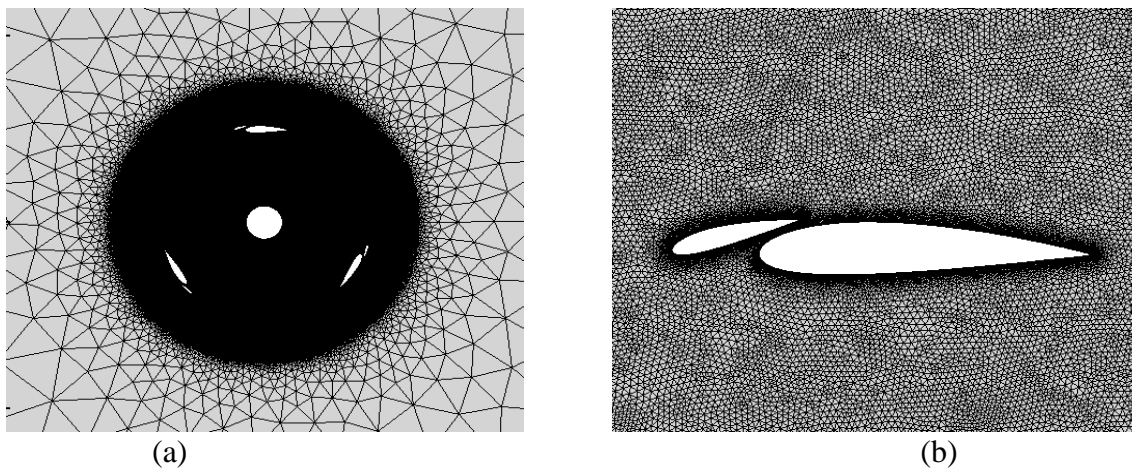


Figure 5: Computational Grid (a) near Rotating Zone (b) near aerofoil and slat

### 3.4. Solution Methods and Controls

Based on results of (8,9) in-compressible un-steady Reynolds Averaged Navier Stokes (URANS), simulations were completed utilizing CFD Commercial version of ANSYS Fluent 16.1 is used. Algorithmic is set based on results of (8). schemes of second-order are used for both spatial and temporal analysis. For pressure and velocity coupling, SIMPLE scheme is employed. Three equation transition SST- turbulence model is utilized for modelling turbulence in accordance with result of (13), which is an improved version over the two-equation  $k-\omega$  SST turbulence model. Laminar-to-turbulent transition model using specified intermittency-based models have shown successful results as shown by Suzen et al.(14,15), Walters and Leylek (16), Cutrone et al. (17) and Genç et al.(18–22) on aerofoils flow, which further enhances the

confidence for these model application. The increment of azimuthal ( $d\theta$ ) used for the validation case are  $1^\circ$ ,  $0.5^\circ$ ,  $0.1^\circ$  and  $0.03^\circ$ . Present study is performed at an azimuth increment of  $0.5^\circ$ . Scaled residual of  $< 1 \times 10^{-5}$  and 20 iterations have been conducted per time step. Coefficient of moment is calculated on 21st revolution of turbine, same values are used for calculating the turbine coefficient of power values are presented in Table 9.

### 3.5. Acoustic Modeling

Aerodynamic noise is either broadband or tonal in nature. They both are strongly dependent on the aerofoil sectional shape, rotor geometry and its surrounding flow conditions. When the airflow passes over the blades aerodynamic noise is typically generated. They can be further categorized into three noise categories: low frequency, Aerofoil self & turbulent inflow noise. The contact between blades and the atmospheric turbulence resulted into turbulent inflow noise which existed in the form of pressure fluxes. Hence responsible for broadband type of noise. Various aerofoil self-noise mechanisms, involving its broadband and tonal and broadband characteristic, (23) are as following:

- Stall Noise
- Noise due to Tip vortex
- Turbulent-boundary-layer trailing edge noise
- Trailing-edge-vortex-shedding noise

Main aim this study is to carry out the comparative analysis of slat size and slat placement angle with respect to aerodynamic & acoustic behavior of the VAWT. In this regard numerical methodology is developed and validated for foreseeing the far-field radiated noise from the turbine blades and comparing the noise level with that of VAWT with slat. The numerical methodology defined earlier is used for predicting aerodynamics and aerodynamic noises and their propagation to far field is calculated using Ffowcs Williams-Hawking (FW-H) model. This model was selected based on available input parameters of the Aeolos-V (1kW) VAWT and results of (24,25). The noise is modeled based on the results of (26). The most generic form of Lighthill acoustic Analogy i.e FW-H equation as presented in (27) is accurate for predicting the arbitrary moving rigid bodies. The inhomogeneous wave equation also called FW-H is deduced from the continuity and Naviere Stokes equations and is explained in detail at (28,29). As per the commercially available data of Aeolos-V (1kW) VAWT, it has a noise level of  $\leq 45$  db (A). In present study, empirical model assuming nonstationary source positions is used in accordance



with (25) for predicting the far field sound pressure level for VAWT. Logarithmic ratio of sound intensity to reference value is calculated by the equation 3.

$$\text{SPL} = L_p = 10 \log[I/I_{\text{ref}}] = 20 \log[p/p_{\text{ref}}] \quad (3)$$

where  $I$  = sound intensity, and equal to  $p_{\text{rms}}^2/(\rho c)$ ;  $p$  = root mean square sound pressure, its reference value for air is  $20 \mu\text{Pa}$ ;  $(\rho c)$  is the specific acoustic impedance of the fluid. Though the model was developed to assess SPL for flows over fixed aerofoil, it is also applicable to rotating blades that operate at high Reynolds number. For all noise sources the empirical relations use directivity angles to represent the directivity and to account for relative position of receiver with respect to trailing or leading edge of aerofoil (30,31). These directivity angles are aligned in azimuth and polar directions of rotor plane and depend on the shifted coordinate system (30–32).

## 4. Validation Study

In order to finalize the methodology, 2D CFD results of Aeolos-V VAWT are compared with experimental data of the Aeolos-V (1kW) Vertical Axis Wind Turbine. Above-mentioned computational setting are used for the validation of reference case. The grid sensitivity analysis was performed for the case. Domain Size, azimuthal angle parameters were selected based on (8). In section 4-6 after adding the slat, grid sensitivity analysis was re-performed and computational setting are defined same as that of the reference case. In present study behavior of VAWT is analyzed on one tip speed ratio. Rotational speed is altered to adjust the faced velocity.

### 4.1. Verification and Validation of Solution

Validation study is performed for VAWT in accordance with result of (8), a numerically steady state result was obtained after 20<sup>th</sup>–21<sup>st</sup> turbine revolution. The study is performed for validation case mentioned in Section 2.5. Details of the same are mentioned below.

- A Mesh sensitivity analysis was performed by selecting coarse, medium, and fine mesh size. The study was based on the percentage difference in CP values for each grid size. Details of mesh sensitivity analysis are presented in Table 5. Based on the result fine mesh was employed in current study.

Quality	Mesh Elements	Reference Case CP
Coarse	203584	0.3446
Medium	278810	0.3416
Fine	335235	0.3408

Table 5: Mesh Independence study for Reference Case

- A time-step independence analysis is carried out which revealed an azimuth increment of  $0.5^\circ$  is enough. Further refinement of the time-step to  $0.1^\circ$  had small effects on CP values and requiring high computational power.

SNO	Revolution / Time step	Reference Cp Value	Error %
1	$1^\circ$	0.3408	-
2	$0.5^\circ$	0.3389	0.55%
3	$0.1^\circ$	0.3356	1.5 %
4	$0.03^\circ$	0.3342	1.93%

Table 6: Time Step Independence Study for Reference Case

To validate the methodology, results of CFD of the reference case are compared with that of operational parameters of Aeolos-V (1kW) VAWT at tip speed ratio ( $\lambda$ ) of 2.094. The CFD results and experimental data at lower tip speed ratio ( $\lambda$ ) 2.094 showed a good agreement, at which dynamic stall causes a complex flow over the turbine blades.

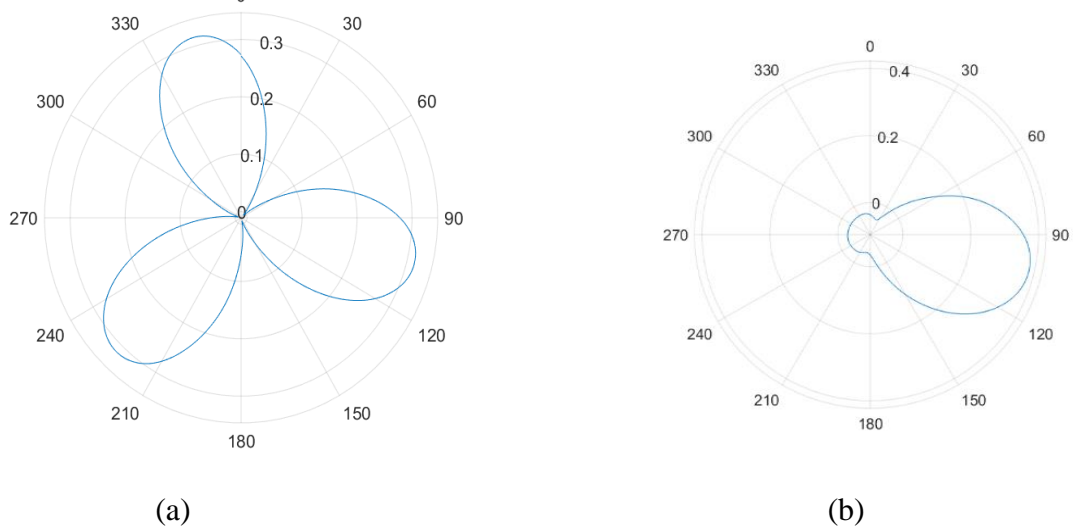


Figure 6 (a): Coefficient of Moment as a function of Azimuth Angle for VAWT. (b) Coefficient of moment of single blade as a function of Azimuth Angle

Figure 6a show the coefficient of moment of VAWT for one complete revolution in polar diagram and 6b represent the coefficient of moment of single turbine blade in polar diagram The

maximum of this function is attained at three different angular positions i.e  $104^\circ$ ,  $224^\circ$ ,  $344^\circ$ . It can be inferred from the polar plot of Single blade that turbine has maximum coefficient of moment at azimuth position of  $104^\circ$ . At this point blade of turbine face a free wind flow which subsequently resulted into maximum torque coefficient. Experimental value of coefficient of power and CFD based coefficient of power of Baseline case of (7) and current study are tabulated in Table 7. There is an overprediction of 9.3 % in current CFD results due to non-capturing of 3D flow effects. The nonconformity between the CFD and experimental data are extensively discussed in (9,33).

Coefficient of Power	CFD Result	Baseline Case (7)	Experimental
	0.3389	0.3500	0.3102

Table 7 Comparison of Coefficient of Power

## 4.2. Acoustic Validation

The polar plot of sound pressure level with azimuth angle are depicted in Figure 7a, which indicate that the radiation of noise is high in the leeward, up & down wind direction ( $90^\circ \sim 270^\circ$ ) and low in the crosswind ( $0^\circ \sim 180^\circ$ ) direction of the observer. The maximum value of the SPL achieved for the reference case is 41 db A which is a good agreement with available noise data of Aeolos-V VAWT. In current study for analyzing the effect of TSPL frequency range of spectrum from 0 to 1200 Hz is selected. TSPL data indicate that maximum sound pressure level at rotor distance of 1.25, 1.75 and 2 is 102 db, 92 and 89 db respectively.

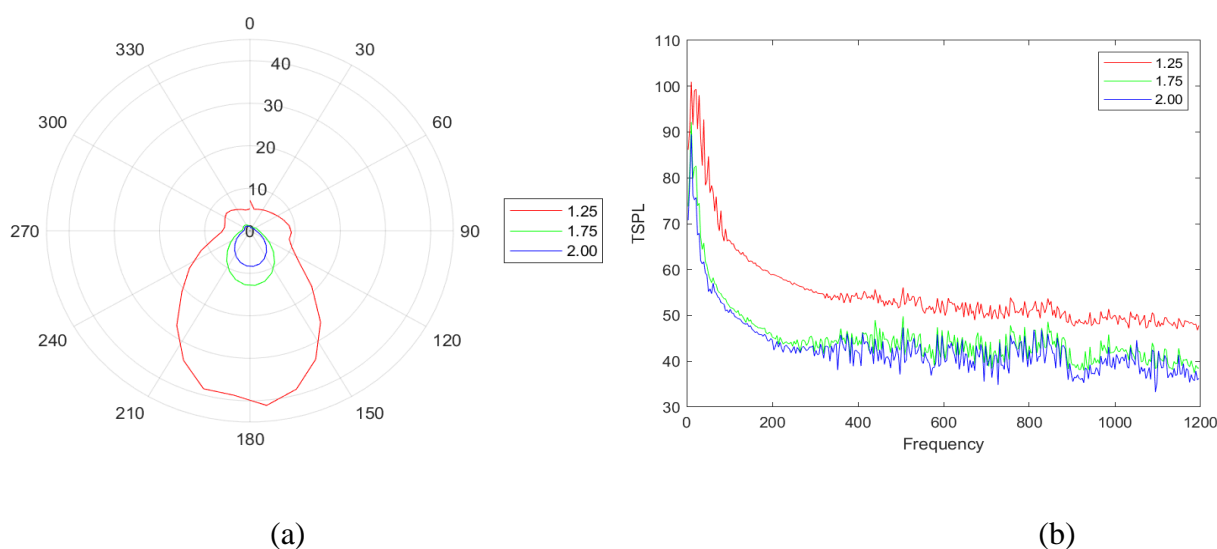


Figure 7 (a) SPL as function of Azimuth Angle, and (b) TSPL as function of Frequency

The data also indicate that the intensity of sound varies logarithmic with distance and has same behavior as of (23). The acoustic results also indicate that intensity of noise decreases by varying

the distance of receiver from turbine however overall behavior of the sound propagation remain same. TSPL curve presented in figure 7 b indicate the peaks in the noise intensity level which decrease with distance from turbine, however the behavior of the intensity curve remains same. The maximum peak of the noise occurred at the lower frequency (30~90 hz) range, results are as per the study of (25). The computed results also showed good agreement with operational noise data of Aeolos -V (1kW) VAWT.

## 5. Aerodynamic and Acoustic behavior of VAWT with Slat

The aerodynamic behavior of Vertical Axis Turbine with Slat has been discussed in succeeding paragraphs.

### 5.1. Numerical Setting

Parametric study on slat size and slat positioning parameters is conducted to achieve optimizes slat size and slat position with overall good aerodynamics and acoustic performance. Study is conducted at tip speed ratio of ( $\lambda$ ) 2.094. Grid Sensitivity analysis was reperformed, uniform reforming of grid is carried out by selecting three grids of coarse, medium and fine quality and values of respective CP values.

Quality	Mesh Element	CP of VAWT with Slat
Coarse	262747	0.1603
Medium	359835	0.1496
Fine	432495	0.1440

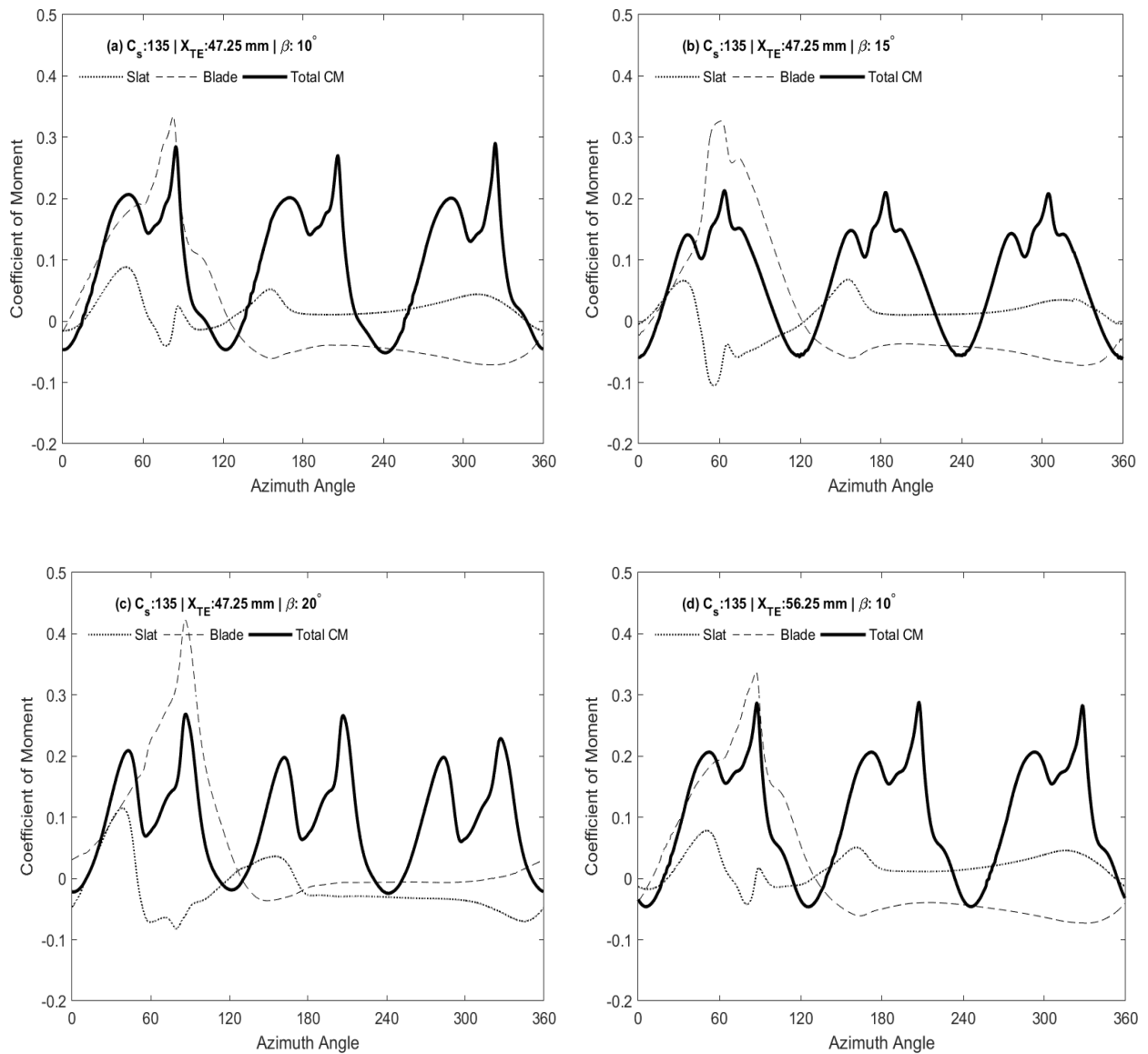
Table 8 : Mesh independence Study for VAWT with Slat

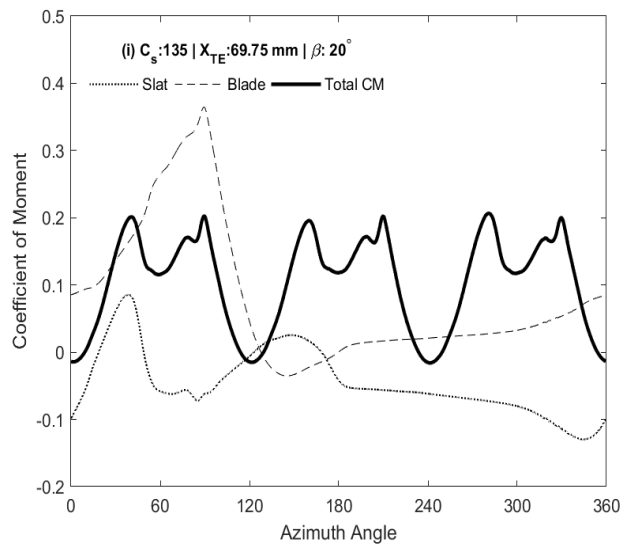
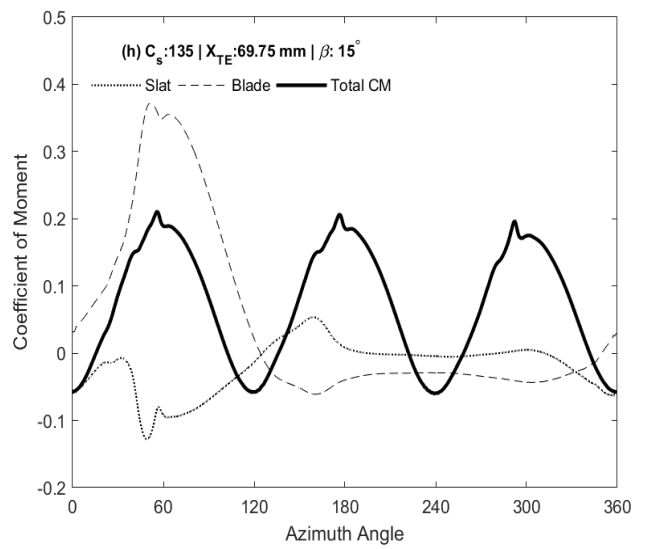
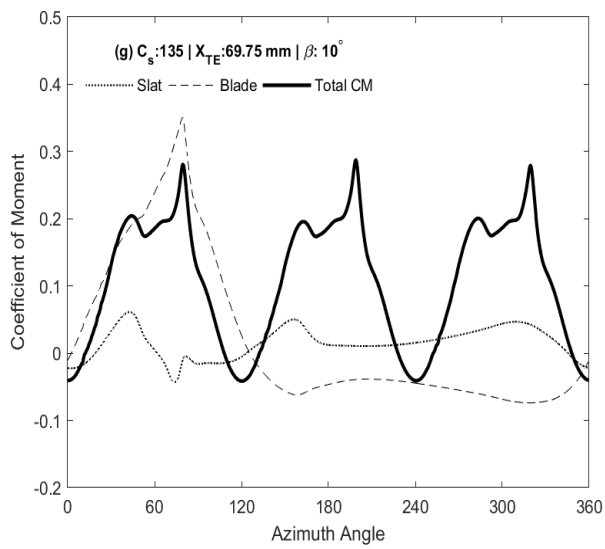
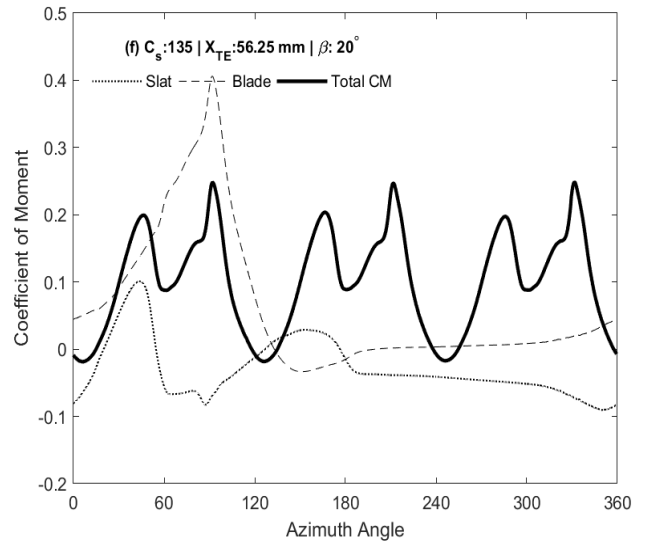
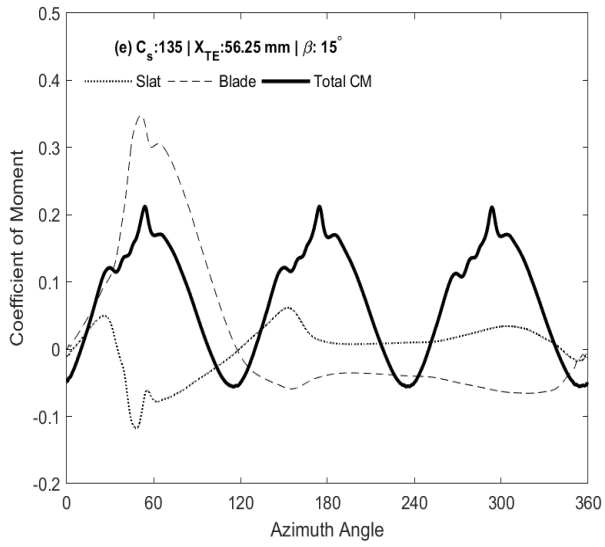
Other computational parameters are kept same. Total number of cells for the VAWT with slat is 4.3 million elements approximately. Slat of three chord length as defined in Table 2 are chosen for CFD analysis. CFD analysis of each slat size is conducted with respect to nine positing parameters described in Table 3. During analysis achieved value of Coefficient of moment of each case of slat size are compared.

### 5.2 Aerodynamics of Slated VAWT

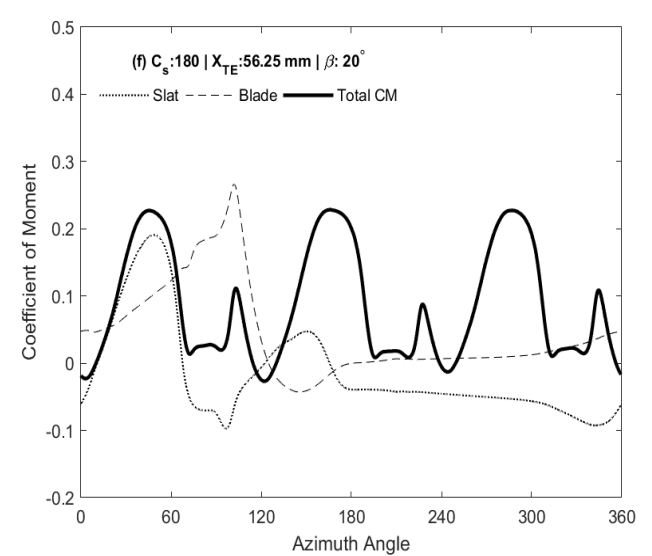
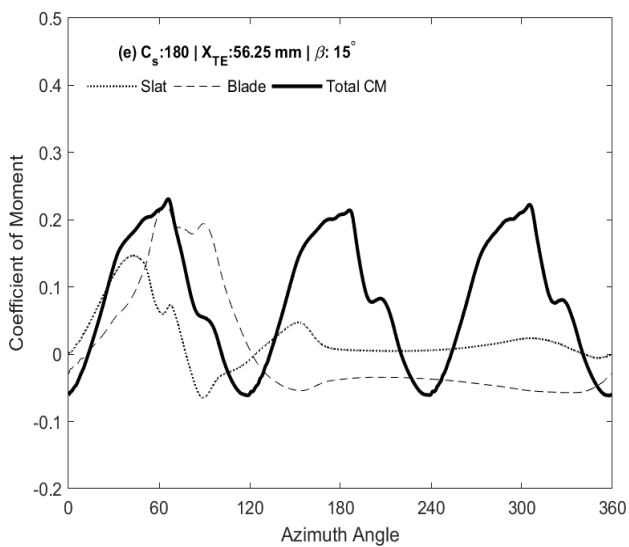
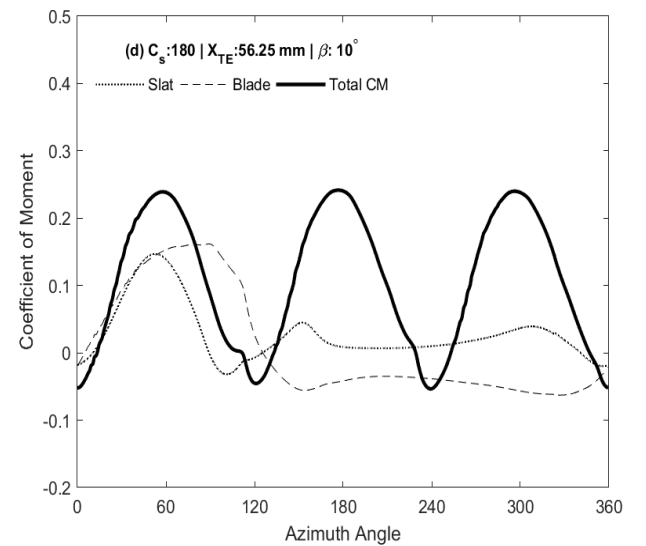
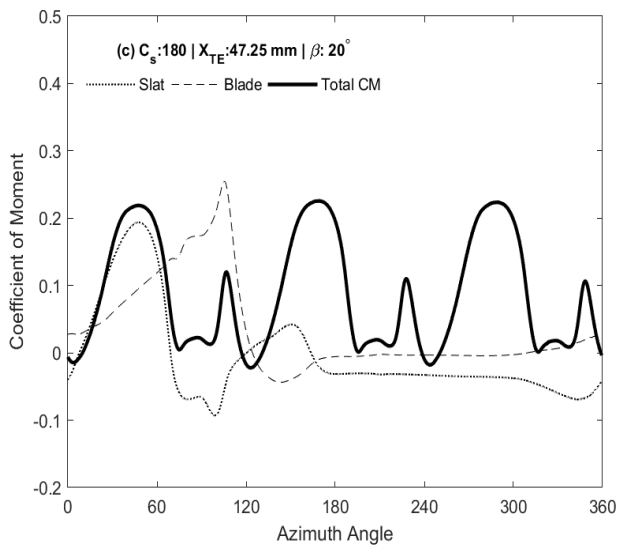
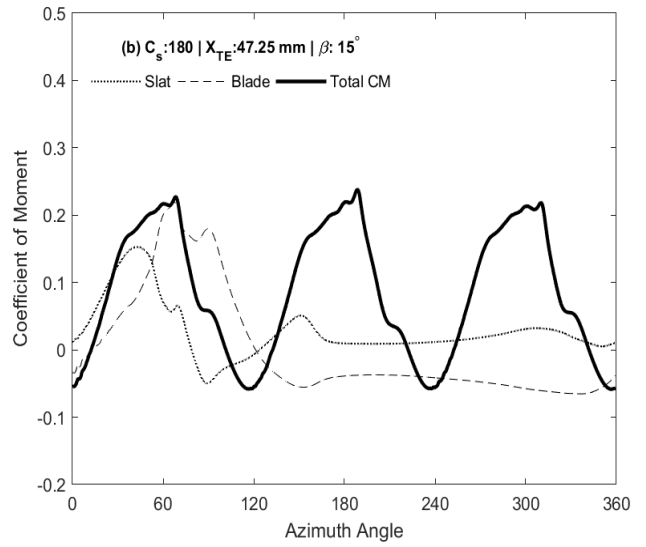
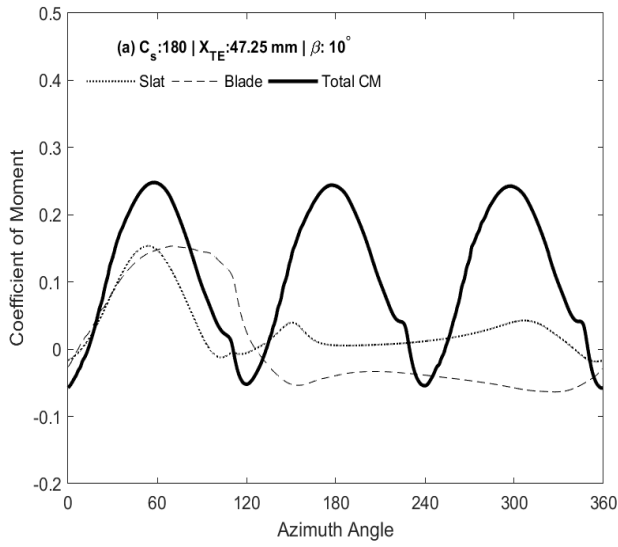
Each slat size is analyzed with respect to nine positioning parameters. The coefficient of moment of VAWT, Blade and Slat for each configuration is studied at corresponding azimuth angle. Figure 8, 9, 10 indicate the coefficient of moment of VAWT with slat, single blade and slat for one complete revolution. Said data indicate that turbine gain maximum instantaneous moment

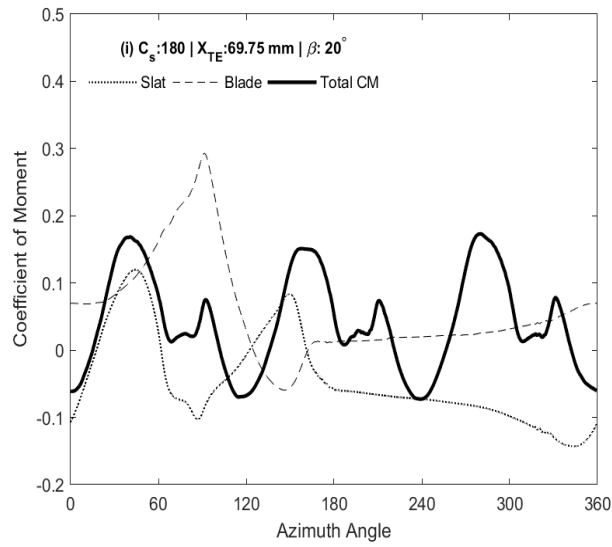
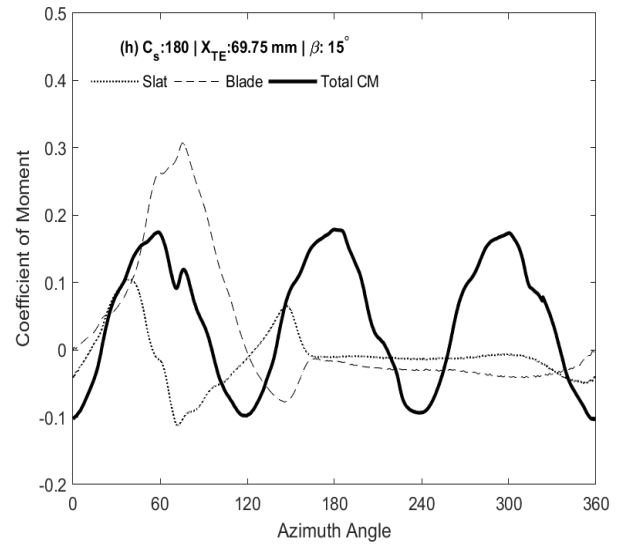
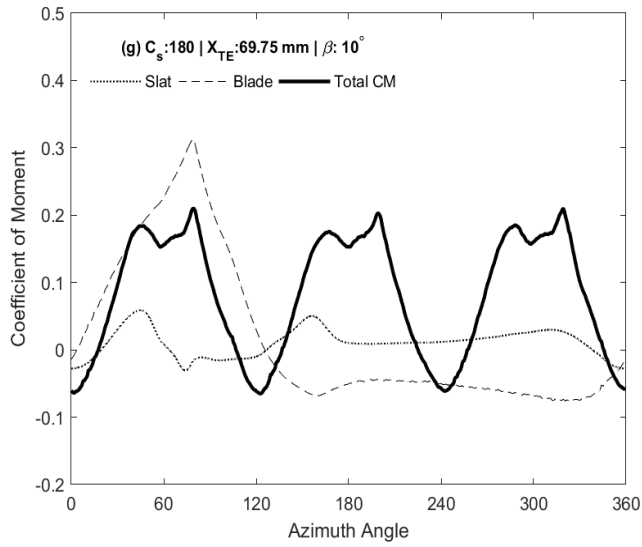
coefficient three times in one revolution. It has been inferred that behavior of moment curve is largely dependent on the slat placement angle ( $\beta$ ) however, amplitude of moment curve is dependent on the slat size and distance of the trailing edge (TE) of the slat aerofoil form leading edge of main aerofoil along the local X-direction. The average moment coefficient achieved for each case is tabulated in Table 9. Maximum value of the CM achieved is 0.1094 for slat size 180mm at slat angle  $10^\circ$  and  $X_{TE}$  47.25 mm.



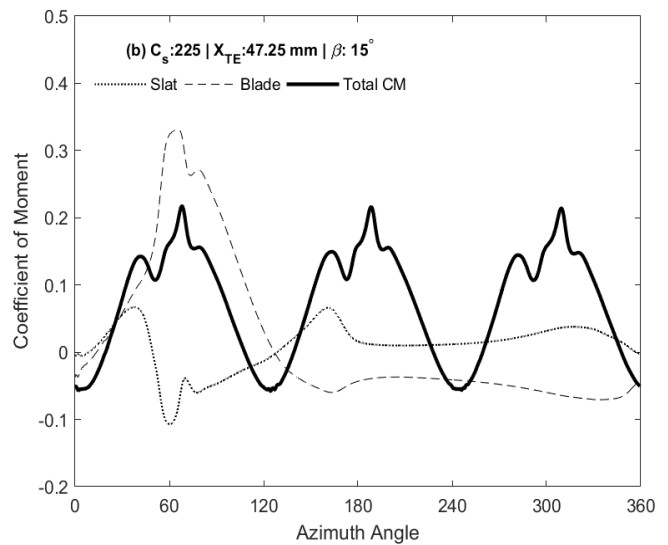
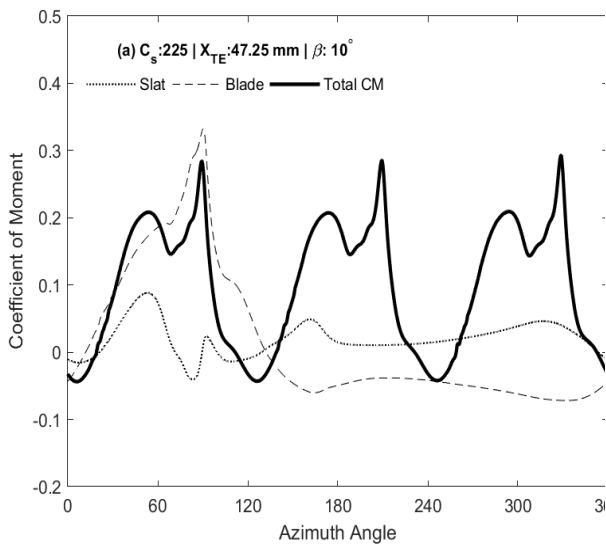


(A)

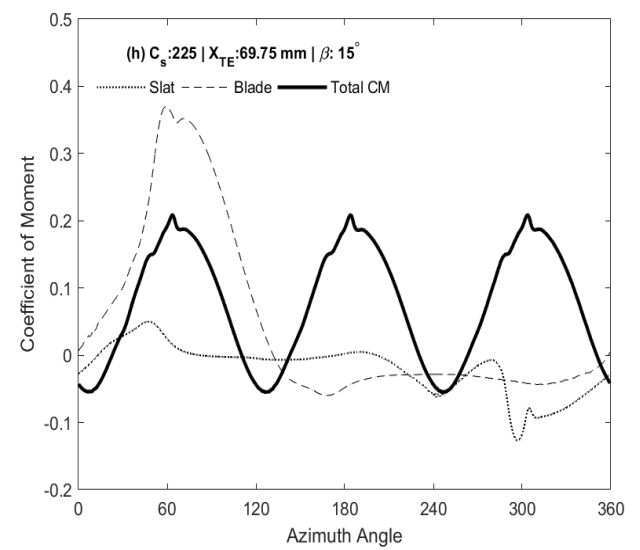
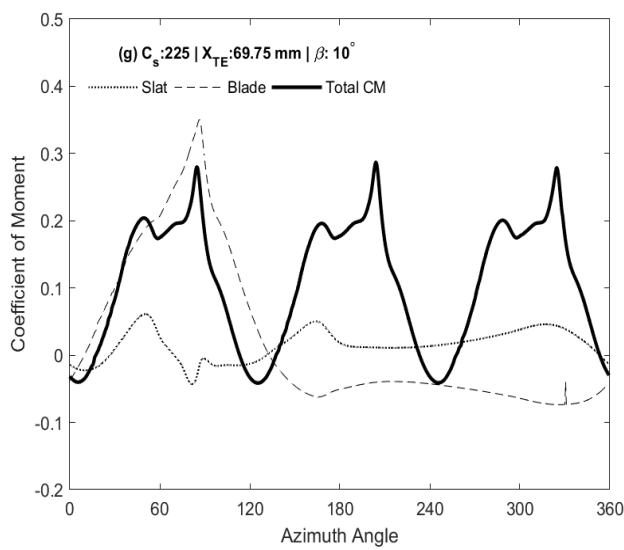
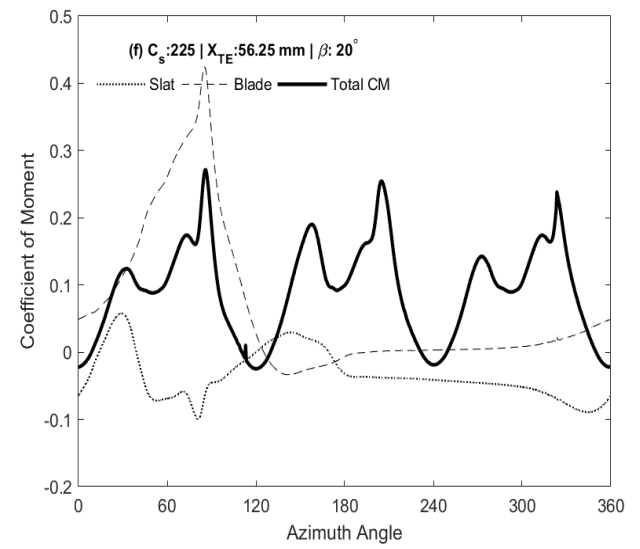
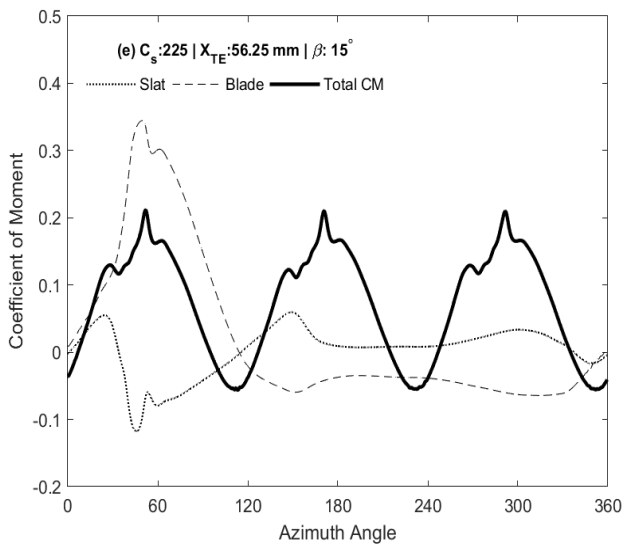
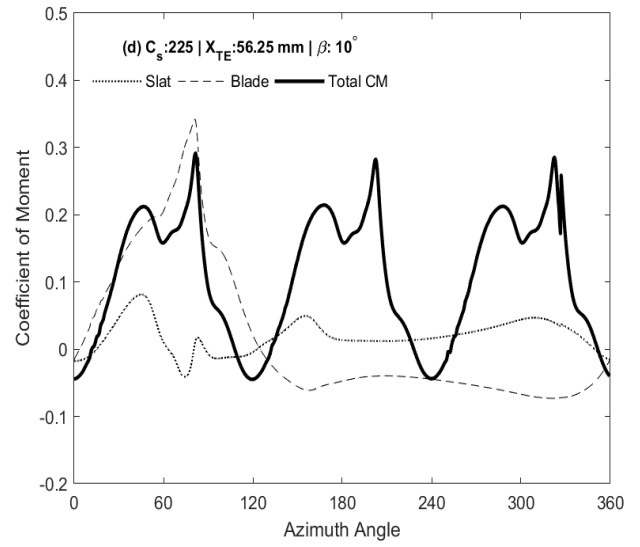
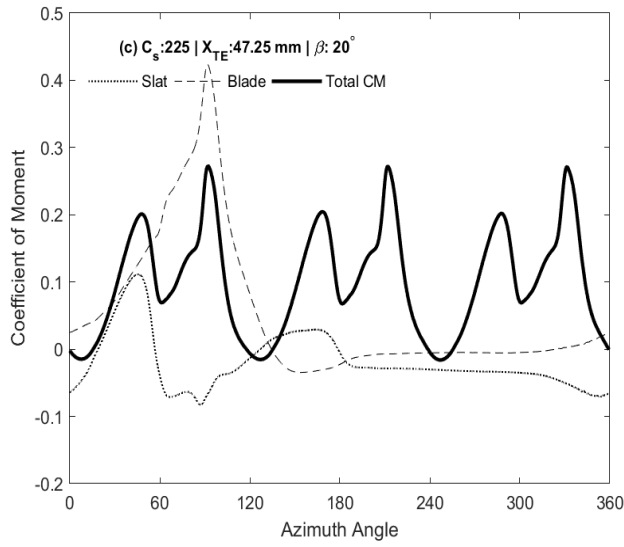


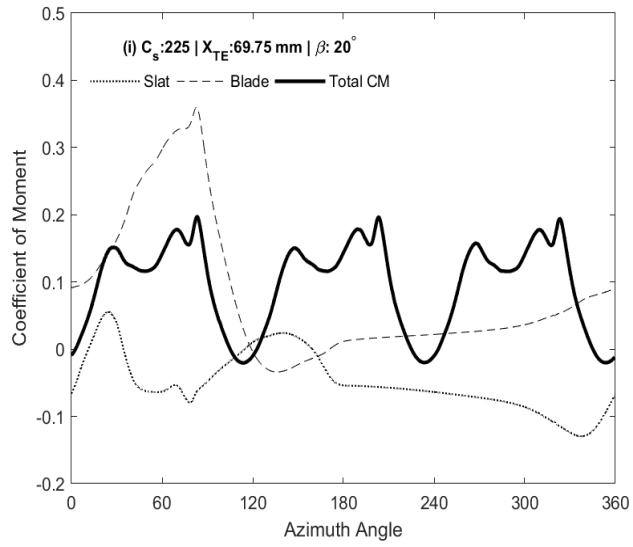


**(B)**









(C)

Figure 8: Coefficient of Moment at different Slat angles and  $X_{TE}$  as function of azimuth angle (A) Slat size 135 mm, (B) Slat Size 180 mm, (C) Slat Size 225 mm

Slat Chord	$X_{TE}$ mm	Angle	Total CM	SPL db (A)
Cs = 135	47.25	10	0.09384	39
		15	0.071251	39
		20	0.0941	43
	56.25	10	0.1025	39
		15	0.0734	39
		20	0.1013	43
	69.75	10	0.1091	39
		15	0.0726	39
		20	0.1053	43
Cs =180	47.25	10	0.1094	40
		15	0.0870	41
		20	0.0874	45
	56.25	10	0.1061	40
		15	0.0817	40
		20	0.0872	44
	69.75	10	0.1090	38
		15	0.0700	40
		20	0.0850	44
Cs =225	47.25	10	0.0996	40
		15	0.0740	39
		20	0.0999	42
	56.25	10	0.1049	41
		15	0.0725	39
		20	0.0923	42
	69.75	10	0.1090	41
		15	0.0773	40
		20	0.0968	42

Table 9: Average value of Moment Coefficient and Maximum value of Sound Pressure Level (SPL db A) at  $x/R$  1.25

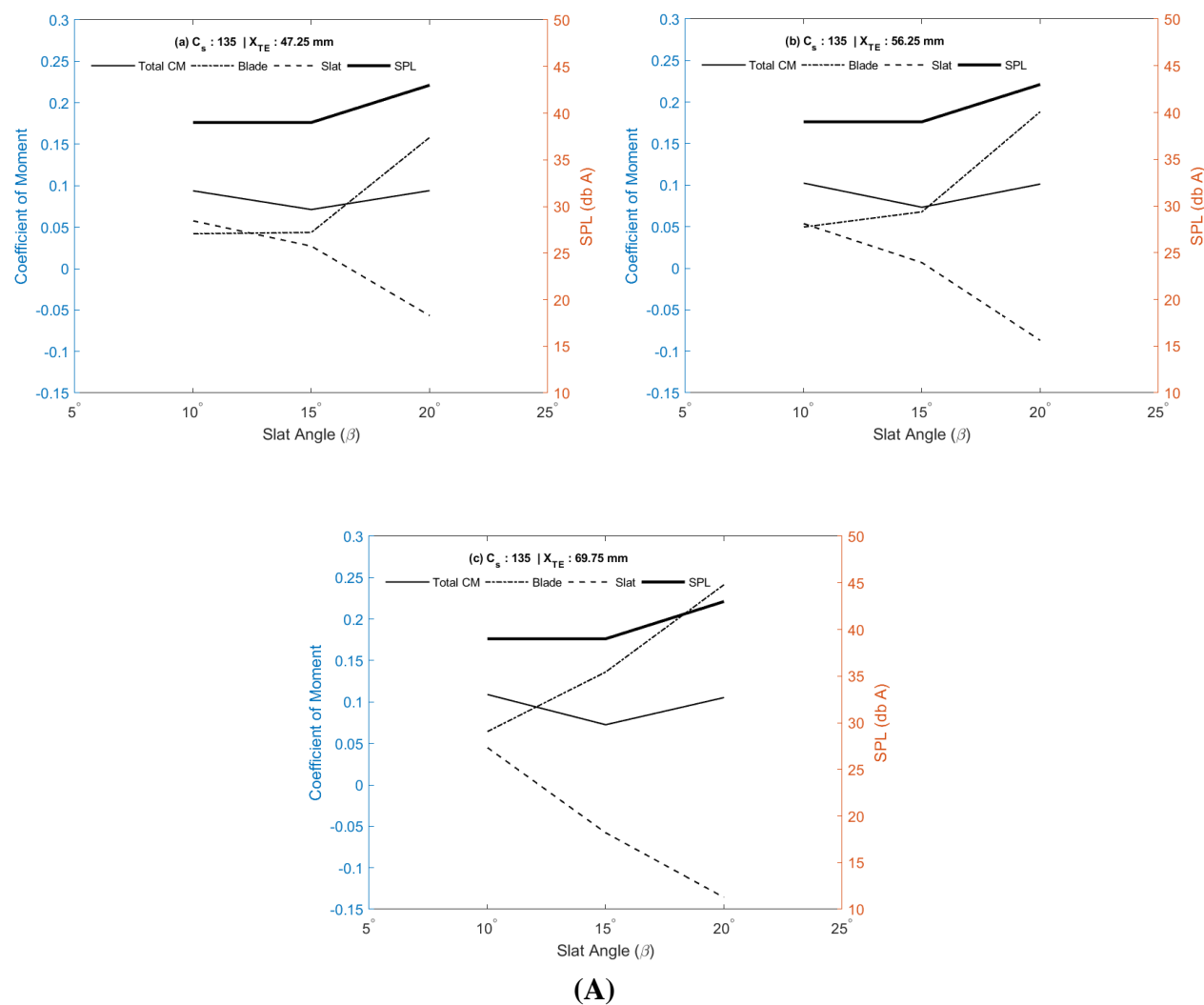
### 5.3 Acoustic of VAWT

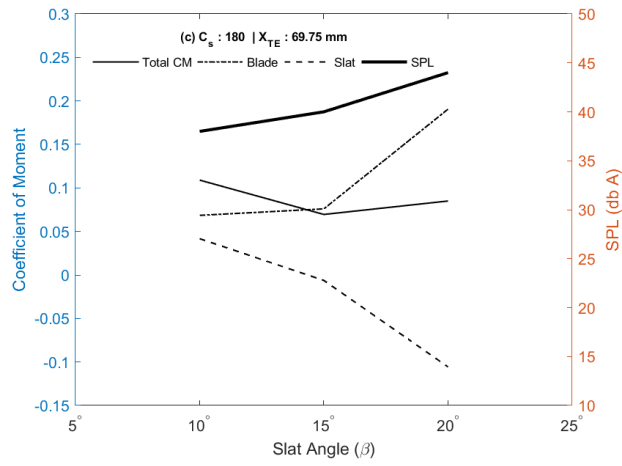
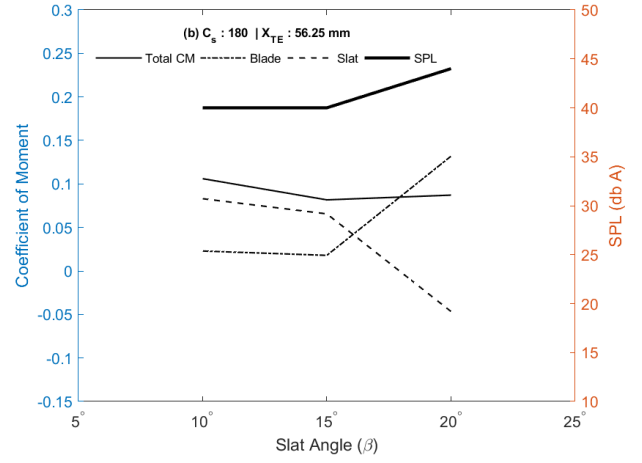
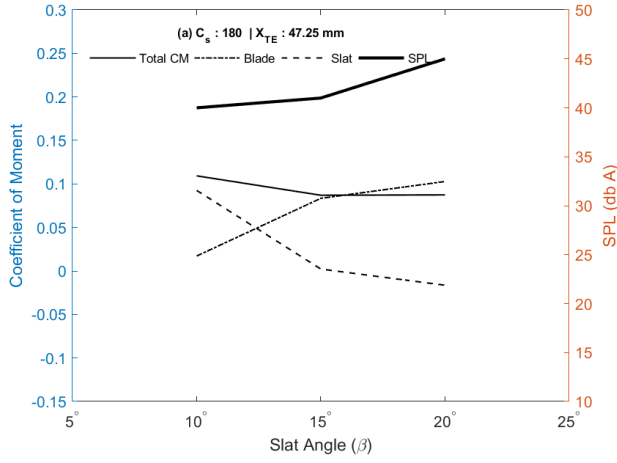
Based on acoustic validation study of VAWT without slat. Comparative analysis of A- weighted Sound power Level of 1/3<sup>rd</sup> octave band of slated VAWT has been carried out. No momentous variation in the acoustic performance of the VAWT with Slat is observed. Said data indicate that the intensity of noise radiated from the turbine is higher in the upwind, downwind leeward wind direction ( $90^\circ \sim 270^\circ$ ) and lower in case of the crosswind direction of the observer and are same as of the study of (3). The total Sound Pressure level (TSPL) as function of frequency at rotor distance  $x/R = 1.25, 1.75$  and  $2$  is depicted in Appendix A. The max value of Sound pressure level at 1.25 of rotor distance is shown in Table 9. The TSPL data at different distances from the turbine indicate a maximum peak value of noise at frequency range of (40~100 Hz). It has been noted from the TSPL curve of VAWT with slat that a small peak in noise at frequency

range of 600~800 Hz similar behavior is noted in all cases. The intensity of noise decreases with increasing the distance from rotor however the behavior of Sound intensity remains the same.

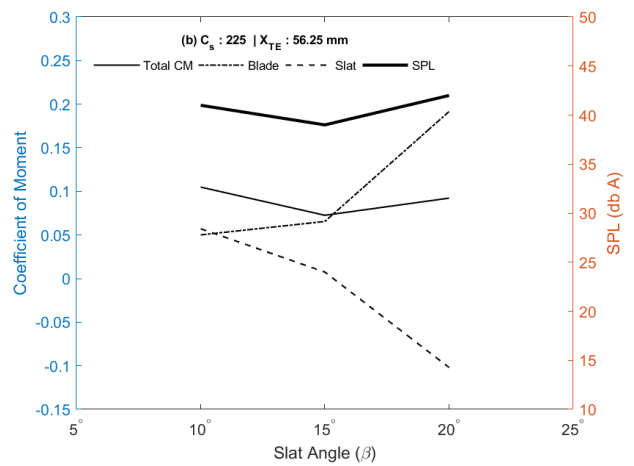
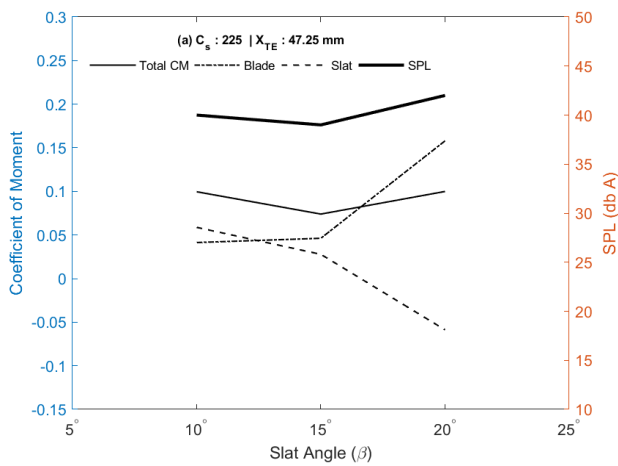
## 5.4. Performance Analysis of VAWT with Slat

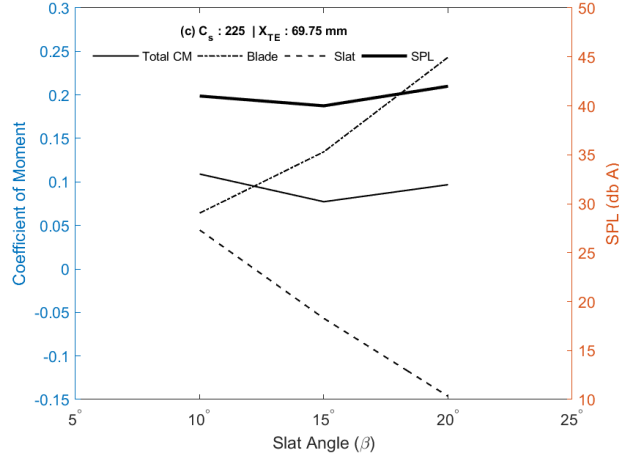
In order to optimize the slat size, slat angle and slat placement parameters a comprehensive analysis of the available aerodynamic and acoustic results has been carried out. On analyzing the behavior of CM curve for one slat size and  $X_{TE}$  it is found that pattern of coefficient of Moment curve is largely dependent on slat angle ( $\beta$ ). On changing the  $X_{TE}$  the amplitude of moment curve changes. It has been noted that main aerofoil is generating more lift whereas slat is generating some amount of negative moment in addition to the positive moment due to stall and wake interaction thus, affecting the overall moment of VAWT. Similarly, the maximum value of A-weighted Sound Pressure Level is also varying with change of Slat Size, Slat angle and  $X_{TE}$ .





**(B)**





(C)

Figure 9: CM & SPL (db A) as a function of Slat Angle (A) Slat Size 135,  $X_{TE} = 47.25, 56.25, 69.75$  mm, (B) Slat Size 180,  $X_{TE} = 47.25, 56.25, 69.75$  mm, (C) Slat Size 225,  $X_{TE} = 47.25, 56.25, 69.75$  mm

Therefore, average CM value of VAWT, main aerofoil and slat along with corresponding maximum values of A-weighted Sound Pressure Level are plotted as a function of slat angle for each  $X_{TE}$  and slat size. The detailed graphs are shown in figure 9 (A, B, C). Abovementioned plot indicate that CM and SPL have overall good value at slat angle  $< 15^\circ$ . On increasing the slat angle beyond  $15^\circ$  the CM of slat decreases exponentially, and SPL increases logarithmically. It has also been noted that total CM of VAWT increases by increasing slat size ( $C_s$ ), moreover, corresponding maximum SPL also increases. From same slat size coefficient of moment decreases by increasing distance between trailing edge of slat aerofoil and leading edge of main aerofoil in X-direction ( $X_{TE}$ ) i.e increasing the overlap of main and slat aerofoil causes decrease in amplitude of coefficient of moment. The aerodynamic and acoustic behavior of VAWT with slat is explained in succeeding paragraphs. The analysis of instantaneous coefficient of moment curve of main aerofoil, slat and slatted VAWT along with the CM and SPL curve revealed following facts about aerodynamics and acoustic behavior of turbine.

## 5.4.1 Behavior of Instantaneous Moment Curve

On analyzing the behavior of CM Curve of VAWT it has been observed that in some cases CM curves have single amplitude peak whereas in few cases curves has dual amplitude peak. Behavior of slat and main aerofoil of these cases is discussed in detail in succeeding paragraphs.

### 5.4.1.1 Single Amplitude Peak in CM Curve

In all cases where amplitude of CM curve has single peak, it has been observed slat is producing the positive moment only moreover, its CM is in phase with the moment of the main aerofoil

refer figure 9 B(a,b,d,e)] thus augmenting the overall instantaneous moment. It is pertinent to note that in all these cases the Slat angle is  $10^\circ$  and  $15^\circ$  respectively. In all these cases slat and main aerofoil are stalling at same angle and overall CM has increased, same behavior is supported by vorticity contours of these cases.

#### **5.4.1.2 Dual Amplitude peaks in CM Curve**

In most of the cases it is observed that CM curve has dual peaks of amplitude and this phenomenon get pronounce with an increment in the slat placement angle refer figure 8 [A, B, C]. In these cases, it is noted that slat is producing the negative moment in addition to the positive moment and negative moment is in phase with the positive moment of main aerofoil thus countering its effect and decreasing the overall instantaneous moment.

#### **5.4.2 Effect of Distance between slat aerofoil trailing edge and leading edge of Main aerofoil in X-direction ( $X_{TE}$ ) on Coefficient of Moment.**

By comparing the average instantaneous coefficient of moment, it was found that Coefficient of moment increases by decreasing the  $X_{TE}$  i.e placing slat more ahead of main aerofoil resulted in an improved Coefficient of moment wrt configuration in which the  $X_{TE}$  is large. Same is evident from the behavior of CM curve of all cases (a, d, g), at high value of  $X_{TE}$  the slat produces more negative moment and counter the effect of main aerofoil thus causing the decrease in overall moment coefficient. Moreover, this behavior pronounce as the slat size increases subsequently the increase in the maximum value of A- weighted Sound Pressure Level was also observed. Refer Figure 8 [A(a,b,c),B(a,b,c), C(a,b,c) ].

#### **5.4.3 Effect of Slat Angle ( $\beta$ )**

Performance of VAWT with slat is greatly dependent on the slat placement angle. It has been observed that at same slat size and  $X_{TE}$ , on increasing the slat placement angle the slat produces more negative moment and thus decreasing the average coefficient of moment of VAWT Refer figure 8 A (c,f,i). It is pertinent to mention that increasing the slat angle resulted in to increase in maximum value of A- weighted Sound Pressure Level due to counter effect of slat and blade moment.

#### 5.4.4 Effect of Slat Size ( $C_s$ )

Slat size has also affected the instantaneous moment. It has been observed that at same  $X_{TE}$  and  $\beta$ , by increasing the slat chord length from 135 mm to 180 mm moment of coefficient increases by 16 percent and increasing chord from 135 to 225 mm resulted in an increase of only 6% in moment coefficient. It is worth highlighting that by increasing the slat size form 135mm to 225 mm corresponding value of A- weighted Sound Pressure Level has also increased logarithmically.

Configuration	Moment Coefficient	Percentage Increase
( $C_s = 135$ , $X_{TE} = 47.25$ mm, $\beta = 10^\circ$ )	0.0938	
( $C_s = 180$ , $X_{TE} = 47.25$ mm, $\beta = 10^\circ$ )	0.1094	16 %
( $C_s = 225$ , $X_{TE} = 47.25$ mm, $\beta = 10^\circ$ )	0.0996	6 %

Table 10: Comparison of Moment Coefficient

By comparing the value of moment coefficient of all slat sizes it is observed that at that maximum value of coefficient moment (0.1094) is achieved at in above-mentioned configuration. In this configuration the value of  $X_{TE}$  and  $\beta$  is 47.25 mm and  $10^\circ$ . The vorticity behavior of this configuration is shown in figure 11.

#### 5.4.5 Sound Pressure Level

The behavior of SPL curve revealed that by adding the slat overall SPL of turbine increases. On increasing the slat size ( $C_s$ ) and slat angle ( $\beta$ ) the A-weighted SPL increases logarithmically however,  $X_{TE}$  has no significant effect on the A-weighted SPL. The increase in A-weighted SPL with slat addition is mainly due to increase in the intensity of aerodynamic noises. Figure 9 a depict the directivity plot of A-weighted SPL and TSPL of configuration where maximum SPL is observed. The TSPL curve indicate a maximum peak at 50-100 Hz. The similar behavior is observed at receiver placed at distance  $x/R = 1.25, 1.75, 2$  from turbine, sound pressure level decreases logarithmically with distance of the observer. In comparison to the TSPL curve of normal VAWT and VAWT with a slat second peak in total sound pressure level is observed at 600 to 800 Hz mainly due to an increase in the intensity of the associated aerodynamic noise



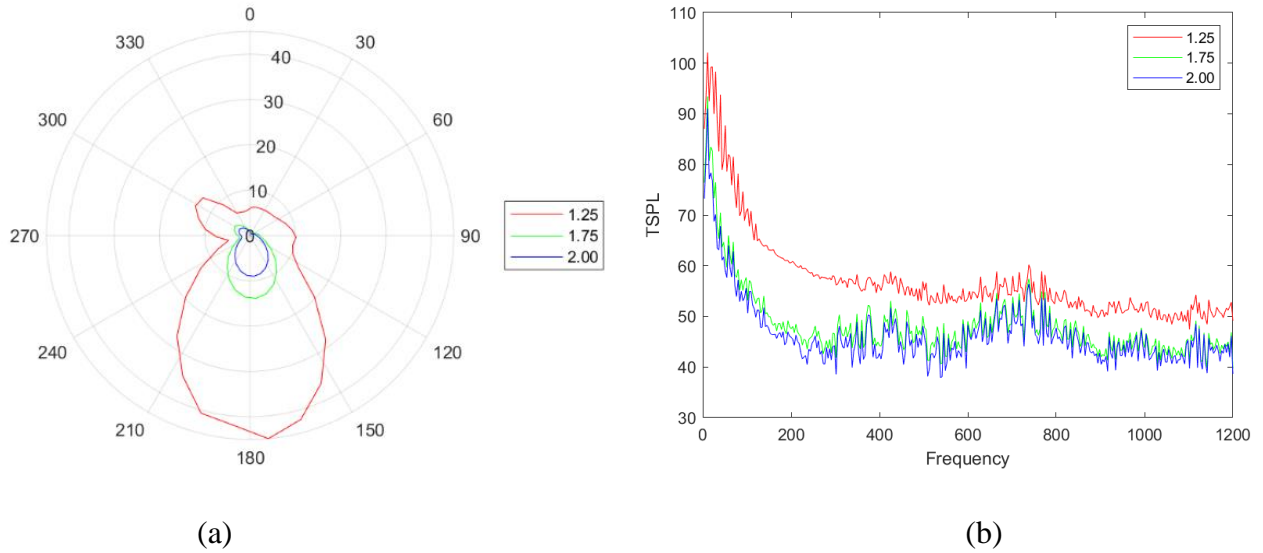


Figure 10: Sound Pressure Level as function of azimuth angle (a) Directivity Plot of A-weighted SPL (b) TSPL Plot at  $x/R = 1.25, 1.75, 2$

## 5.4.6 Vorticity Curve of Case with Slat angle $10^\circ$ & $20^\circ$

The present model accurately predicts the wake effects and dynamic stall of VAWT. Interaction of dynamic stall vortices and Trailing edge vortices resulted in the complex flow field. Arguments mentioned in para 2,3, 4 & 5 above are also supported by the vorticity curve of these cases. Contours of vorticity magnitude at  $\lambda = 2.094$  for two cases one with max CM and low SPL and other one with low CM and comparatively high SPL are discussed here.

### 5.4.6.1 Max CP and low SPL

Firstly, the performance of case in which maximum instantaneous moment achieved is discussed. The vorticity behavior of VAWT at azimuth angle  $56.5^\circ$  and  $120^\circ$  (where maximum and minimum magnitude of CM curve is achieved) is depicted in figure 9 a & b. At Max performance of VAWT behavior of slat and main aerofoil are in phase and augmenting the moment of each other. Moreover, all blades are producing some amount of positive moment thus achieving maximum instantaneous moment. In this case due to no negative or counter moment effect of blades intensity of aerodynamic noise radiated from VAWT are also less. In present case blade-blade flow interaction are coupled. There is direct effect of wake of slat on main aerofoil. Rear element is directly affected by the trailing edge vortex of front element and leading-edge vortex

is also affecting its flow field to some extent. In this case vortex-vortex interaction resulted in flow reattachment and thus augmenting the moment coefficient.

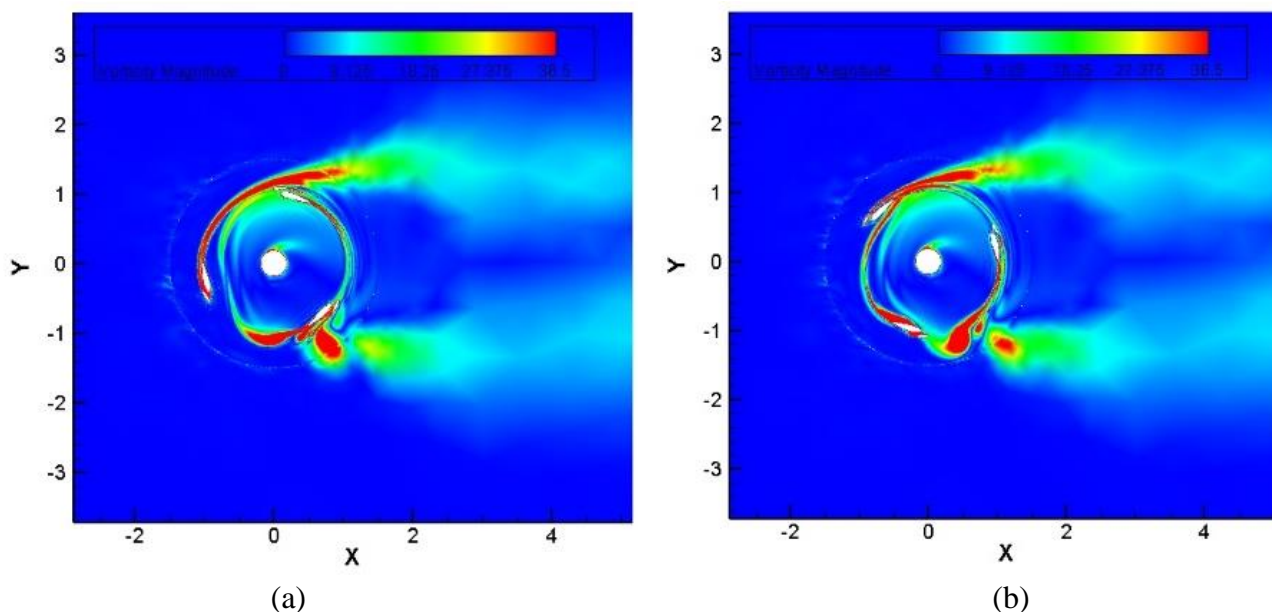


Figure 11: Vorticity contours of ( $C_s = 180$ ,  $X_{TE} = 47.25$  mm,  $\beta = 10^\circ$ ) at Max (a) and Min (b) Performance

It has been inferred from the vorticity contours in upstream region that:

- The vortex interaction in this case are favoring the reattachment of the flow.
- The equivalent blade length (including main aerofoil and slat chord) has an overall attached flow
- Similar features reappear in the downstream section, but it is not as manifest as is in the case of upstream.

#### 5.4.6.2 Max CP and High SPL

In second case as per the behavior of CM curve, slat is generating the negative moment in addition to generating positive moment. Thus, overall CM of VAWT decreases in comparison to max performance case. It is pertinent to note that maximum value of SPL is achieved in this case. At high slat angle this phenomenon gets pronounced. Same is evident from the vorticity contours of VAWT at maximum and minimum CM angles. Refer figure 10 (a) & (b). It has been inferred from the vorticity contours in upstream region that:

- The vortex interaction in this case are not favoring the reattachment of the flow.
- The equivalent blade length (including main aerofoil and slat chord) has an overall no attached flow
- Similar features reappear in the downstream section with dominant affect.

- Due to the additional flow detachment effect of slat Sound Pressure level of this case is high.

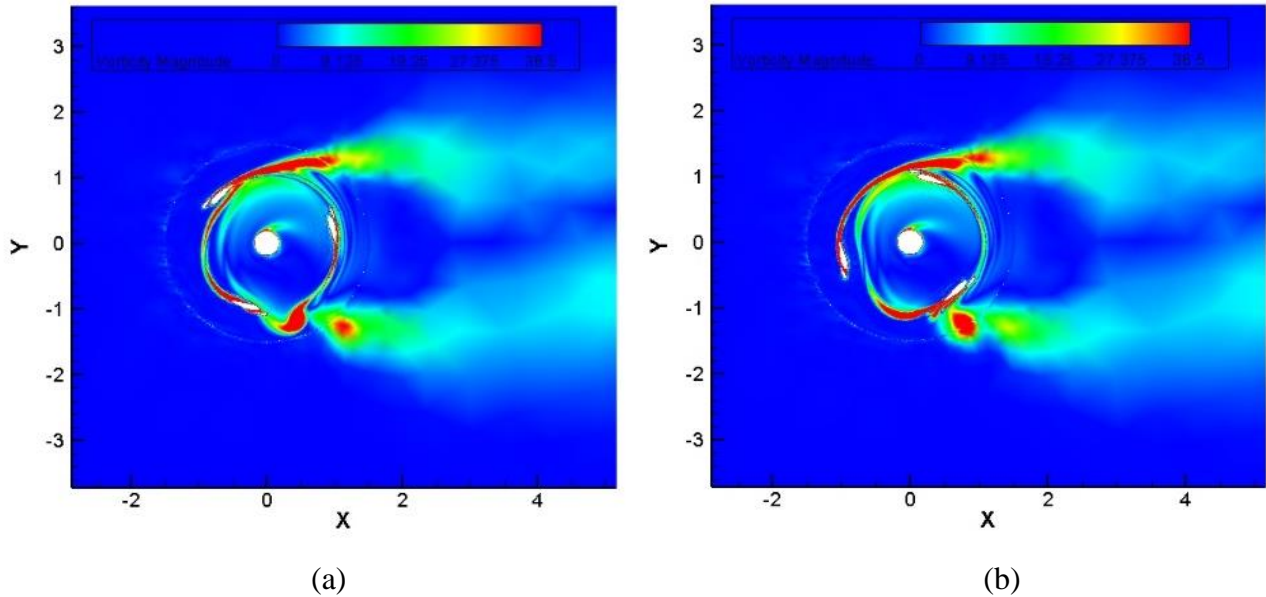


Figure 12: Vorticity contours of ( $C_s = 180$ ,  $X_{TE} = 47.25$  mm,  $\beta = 20^\circ$ ) at Max (a) and Min (b) Performance

## 6. Discussion

In current study CFD results for all the parameters are examined at 21st turbine revolution (8). Result of CFD simulations are validated with the available operational and technical data of Aeolos-V (1kW) VAWT. Note that the present study is performed using the fine azimuth increase  $d\theta$  of  $0.5^\circ$ , this value is accurate for derived minimum requirement of current  $\lambda$  value and was calculated based on the results of (8). The Slat sizing and Slat placement parameters were selected as per the guidelines of (4,10,11). The acoustic formulation is based on the result of (23,25). A good agreement in CFD result was observed at  $\lambda$  of 2.094. The acoustic data of the VAWT with and without the slat indicate that the intensity of the sound decrease with increasing the distance from the turbine however, the variation is logarithmic and same behavior of sound followed at receiver placed at different distances from turbine. It is worth mentioning that performance of VAWT with slat at other tip speed ratio  $\lambda$  may be dedicatedly performed as part of future research.

### 6.1 Recommendation for future Work

After reviewing the results of the performed simulations and previous literature, following recommendations are made:

- Performance of VAWT with slat may be studied at other tip speed ratios
- 3D simulation of the VAWT with slat may be conducted.

- Experimental validation of the CFD simulation and acoustic noise calculation may be carried out.

## 7. Conclusion

Computational analysis was conducted using URANS simulations to predict the aerodynamic behavior of Aeolos-V (1kW) VAWT with and without slat. The basic solution of Ffowcs. Williams-Hawkings (FW-H) equation is used for predicting the noise radiating from the far field. The CFD result indicate that the to get the overall good performance of the slatted VAWT, Slat placement angle must be selected  $<15^\circ$  and overlapping of slat and main aerofoil must be set to minimum (10.5 % of main chord). As far as slat size is considered there must be a tradeoff between performance and acceptable noise level of VAWT. The vorticity curve also supports the argument that when the overlapping of main and slat aerofoil is less flow reattachment phenomenon is significant which get more pronounced at relatively small slat placement angle ( $\beta$ ). The results also indicate at a given rotating speed the strength of radiated noise from VAWT is decreasing logarithmic by increasing the distance between receiver and turbine. The data of A- weighted sound power level indicate a rise in noise emission from the VAWT to trailing edge noise which also get pronounced with increasing the slat size and slat placement angle.

## References:

1. Almohammadi KM, Ingham DB, Ma L, Pourkashan M. Computational fluid dynamics (CFD) mesh independency techniques for a straight blade vertical axis wind turbine. *Energy*. 2013;
2. Raciti Castelli M, Englaro A, Benini E. The Darrieus wind turbine: Proposal for a new performance prediction model based on CFD. *Energy*. 2011;
3. Mohamed MH. Performance investigation of H-rotor Darrieus turbine with new airfoil shapes. *Energy*. 2012;
4. Gaunaa M, Sørensen NN BC. Thick Multiple Element Airfoils for use on the Inner Part of Wind Turbine Rotors. In: *Torque 2010: The science of making torque from wind* European Wind Energy Association (EWEA) 2010. 2010. p. 135–52.
5. Wagner S., Bareiß R. GG. Noise Mechanisms of Wind Turbines. In: *Wind Turbine Noise*. In: *Wind Turbine Noise*. 1996. p. pp 67-92.
6. Tadamasa A, Zangeneh M. Numerical prediction of wind turbine noise. *Renew Energy*. 2011;
7. Ullah T, Javed A, Abdullah A, Ali M, Uddin E. Computational evaluation of an optimum leading-edge slat deflection angle for dynamic stall control in a novel urban-scale vertical axis wind turbine for low wind speed operation. *Sustain Energy Technol Assessments*. 2020;
8. Rezaeiha A, Montazeri H, Blocken B. Towards accurate CFD simulations of vertical axis wind turbines at different tip speed ratios and solidities: Guidelines for azimuthal increment, domain size and convergence. *Energy Convers Manag*. 2018;
9. Rezaeiha A, Kalkman I, Blocken B. CFD simulation of a vertical axis wind turbine operating at a moderate tip speed ratio: Guidelines for minimum domain size and azimuthal increment. *Renew Energy*. 2017;
10. Chougule P, Nielsen SRK. Simulation of flow over double-element airfoil and wind tunnel test for use in vertical axis wind turbine. In: *Journal of Physics: Conference Series*. 2014.
11. Corporation MD, Beach L. *High-Lift Aerodynamics*. 1975;12(6).
12. Ferreira CS. The near wake of the VAWT 2D and 3D views of the VAWT aerodynamics. *TU Delft Thesis*. 2009;
13. Dhakal TP, Walters DK. A Three-equation variant of the SST k-w model sensitized to rotation and curvature effects. *J Fluids Eng Trans ASME*. 2011;
14. Suzen YB, Huang PG, Hultgren LS, Ashpis DE. Predictions of separated and transitional boundary layers under low-pressure turbine airfoil conditions using an intermittency transport equation. *J Turbomach*. 2003;
15. Suzen YB, Huang PG. Modeling of flow transition using an intermittency transport equation. *J Fluids Eng Trans ASME*. 2000;
16. Walters DK, Leylek JH. A new model for boundary layer transition using a single-point RANS approach. *J Turbomach*. 2004;
17. Cutrone L, De Palma P, Pascazio G, Napolitano M. Predicting transition in two- and three-

- dimensional separated flows. *Int J Heat Fluid Flow*. 2008;
18. Genç MS. Numerical simulation of flow over a thin aerofoil at a high Reynolds number using a transition model. *Proc Inst Mech Eng Part C J Mech Eng Sci*. 2010;
  19. Genç MS, Kaynak Ü, Yapici H. Performance of transition model for predicting low Re aerofoil flows without/with single and simultaneous blowing and suction. *Eur J Mech B/Fluids*. 2011;
  20. Genç MS, Kaynak Ü, Lock GD. Flow over an aerofoil without and with a leading-edge slat at a transitional Reynolds number. *Proc Inst Mech Eng Part G J Aerosp Eng*. 2009;
  21. Genç MS, Karasu I, Hakan Açikel H. An experimental study on aerodynamics of NACA2415 aerofoil at low Re numbers. *Exp Therm Fluid Sci*. 2012;
  22. M. Serdar Genc IK. Numerical Study on Low Reynolds Number Flows Over an Aerofoil. *J Appl Mech Eng*. 2013;
  23. Ghasemian M, Nejat A. Aero-acoustics prediction of a vertical axis wind turbine using Large Eddy Simulation and acoustic analogy. *Energy*. 2015;
  24. Afanasieva N. The Effect of Angle of Attack and Flow Conditions on Turbulent Boundary Layer Noise of Small Wind Turbines. *Arch Acoust*. 2017;
  25. Bhargava V, Samala R. Acoustic emissions from wind turbine blades. *J Aerosp Technol Manag*. 2019;
  26. WILLIAMS JEF, HAWKINGS DL. SOUND GENERATION BY TURBULENCE AND SURFACES IN ARBITRARY MOTION. *Roy Soc London-Philosophical Trans Ser A*. 1969;
  27. On sound generated aerodynamically I. General theory. *Proc R Soc London Ser A Math Phys Sci*. 1952;
  28. Morris PJ, Long LN, Brentner KS. An aeroacoustic analysis of wind turbines. In: *Collection of ASME Wind Energy Symposium Technical Papers AIAA Aerospace Sciences Meeting and Exhibit*. 2004.
  29. Di Franciscantonio P. A new boundary integral formulation for the prediction of sound radiation. *J Sound Vib*. 1997;
  30. Pope D. Airfoil self-noise and prediction *Airfoil Self-Noise and Prediction*. 2016;(August 1989).
  31. Moriarty P, Migliore P. Semi-empirical aeroacoustic noise prediction code for wind turbines. *National Renewable Energy Laboratory (NREL)*. 2003.
  32. Zhu WJ. *IMPORTANT\_Model of noise of wind turbine blade.pdf*. 2004;
  33. Rezaeiha A, Kalkman I, Blocken B. Effect of pitch angle on power performance and aerodynamics of a vertical axis wind turbine. *Appl Energy*. 2017;

# Thesis Report

## ORIGINALITY REPORT

12%

SIMILARITY INDEX

6%

INTERNET SOURCES

9%

PUBLICATIONS

6%

STUDENT PAPERS

## PRIMARY SOURCES

1	<b>windharvest.com</b> Internet Source	2%
2	Vasishta Bhargava, Rahul Samala. "Acoustic Emissions from Wind Turbine Blades", Journal of Aerospace Technology and Management, 2019 Publication	2%
3	Submitted to Higher Education Commission Pakistan Student Paper	1%
4	Abdolrahim Rezaeiha, Hamid Montazeri, Bert Blocken. "Towards accurate CFD simulations of vertical axis wind turbines at different tip speed ratios and solidities: Guidelines for azimuthal increment, domain size and convergence", Energy Conversion and Management, 2018 Publication	1%
5	<b>worldwidescience.org</b> Internet Source	1%

  
DR. EMAD UDDIN

HoD Mech Engg.  
School of Mechanical &  
Manufacturing Engineering (SMME)  
NUST, H-12, Islamabad

6

Internet Source

&lt;1%

7

Submitted to Indian Institute of Technology  
Guwahati

Student Paper

&lt;1%

8

Abdolrahim Rezaeiha, Ivo Kalkman, Bert  
Blocken. "Effect of pitch angle on power  
performance and aerodynamics of a vertical axis  
wind turbine", Applied Energy, 2017

Publication

&lt;1%

9

Submitted to University of Southampton

Student Paper

&lt;1%

10

Submitted to The University of Manchester

Student Paper

&lt;1%

11

Submitted to British University in Egypt

Student Paper

&lt;1%

12

Townend, H. C. H.. "A Study of Slots, Rings &  
Boundary Layer Control by Blowing", Journal of  
the Royal Aeronautical Society, 1931.

Publication

&lt;1%

13

[www.mdpi.com](http://www.mdpi.com)

Internet Source

&lt;1%

14

Tadamasa, A.. "Numerical prediction of wind  
turbine noise", Renewable Energy, 201107

Publication

&lt;1%



15

Submitted to University of South Australia

Student Paper

&lt;1%

16

Submitted to Oxford Brookes University

Student Paper

&lt;1%

17

Eric Loth, Adam Steele, Chao Qin, Brian Ichter, Michael S. Selig, Patrick Moriarty. "Downwind pre-aligned rotors for extreme-scale wind turbines", Wind Energy, 2017

Publication

&lt;1%

18

[journals.sagepub.com](http://journals.sagepub.com)

Internet Source

&lt;1%

19

Hashem, I., M.H. Mohamed, and A.A. Hafiz. "Aero-acoustics noise assessment for Wind-Lens turbine", Energy, 2017.

Publication

&lt;1%

20

[www.jrors.ir](http://www.jrors.ir)

Internet Source

&lt;1%

21

Lam, H.F., and H.Y. Peng. "Study of wake characteristics of a vertical axis wind turbine by two- and three-dimensional computational fluid dynamics simulations", Renewable Energy, 2016.

Publication

&lt;1%

22

Alessandro Zanon, Pietro Giannattasio, Carlos J. Simão Ferreira. "Wake modelling of a VAWT

&lt;1%

# in dynamic stall: impact on the prediction of flow and induction fields", Wind Energy, 2015

Publication

23

[arc.aiaa.org](http://arc.aiaa.org)

Internet Source

<1%

24

[vbn.aau.dk](http://vbn.aau.dk)

Internet Source

<1%

25

Submitted to University of the Highlands and Islands Millennium Institute

Student Paper

<1%

26

Mohamed Ould Moussa. "Experimental and numerical performances analysis of a small three blades wind turbine", Energy, 2020

Publication

<1%

27

Submitted to Gaziantep Aniversitesi

Student Paper

<1%

28

Submitted to The Hong Kong Polytechnic University

Student Paper

<1%

29

Submitted to Monash University

Student Paper

<1%

30

[www.conserve-energy-future.com](http://www.conserve-energy-future.com)

Internet Source

<1%

31

Submitted to Amrita Vishwa Vidyapeetham

Student Paper

<1%

32

Abdolrahim Rezaeiha, Hamid Montazeri, Bert Blocken. "On the accuracy of turbulence models for CFD simulations of vertical axis wind turbines", Energy, 2019

Publication

<1%

33

Chougule, Prasad, and Søren R K Nielsen. "Simulation of flow over double-element airfoil and wind tunnel test for use in vertical axis wind turbine", Journal of Physics Conference Series, 2014.

Publication

<1%

34

Yunus Celik, Lin Ma, Derek Ingham, Mohamed Pourkashanian. "Aerodynamic investigation of the start-up process of H-type vertical axis wind turbines using CFD", Journal of Wind Engineering and Industrial Aerodynamics, 2020

Publication

<1%

35

[link.springer.com](https://link.springer.com)

Internet Source

<1%

36

Jian Liu, Weiyang Qiao, Wenhua Duan. "Effect of Bowed/Leaned Vane on the Unsteady Aerodynamic Excitation in Transonic Turbine", Journal of Thermal Science, 2018

Publication

<1%

37

Vanhollebeke, F., J. Peeters, D. Vandepitte, and W. Desmet. "Using transfer path analysis to assess the influence of bearings on structural

<1%

vibrations of a wind turbine gearbox : Using TPA to assess the influence of bearings on WT gearbox vibrations", Wind Energy, 2014.

Publication

---

38

royalsocietypublishing.org

Internet Source

<1%

---

39

Submitted to University of Huddersfield

Student Paper

<1%

---

40

Tummala, Abhishiktha, Ratna Kishore Velamati, Dipankur Kumar Sinha, V. Indraja, and V. Hari Krishna. "A review on small scale wind turbines", Renewable and Sustainable Energy Reviews, 2016.

Publication

<1%

---

41

Submitted to Kensington College of Business

Student Paper

<1%

---

42

Advanced Structured Materials, 2013.

Publication

<1%

---

43

Masoud Ghasemian, Amir Nejat. "Aero-acoustics prediction of a vertical axis wind turbine using Large Eddy Simulation and acoustic analogy", Energy, 2015

Publication

---

<1%

---

Exclude quotes Off

Exclude matches Off

Exclude bibliography On